Synthesis and characterization of scalable high permittivity core-shell ferroelectric polymers for energy storage solutions

A Thesis

Presented to

the Faculty of the Department of Electrical and Computer Engineering

University of Houston

In Partial Fulfillment

of the Requirements for the Degree of

Master of Science

in Electrical Engineering

by

Rakesh Mekala

December 2013

Synthesis and characterization of scalable high permittivity core-shell ferroelectric polymers for energy storage solutions

Rakesh Mekala

Approved:

Chair of the Committee
Dr. Alex Ignatiev,
Hugh Roy and Lillie Cranz Cullen Professor of Electrical and Computer Engineering and Physics, Director, Center for Advanced Materials, University of Houston

Committee Members:

Dr. Nacer Badi,
Research Associate Professor,
Physics

Dr. Alex Freundlich,
Research Professor,
Electrical and Computer Engineering and Physics

Dr. Suresh Khator,
Associate Dean,
Cullen College of Engineering

Dr. Francisco C Robles-Hernandez,
Assistant Professor,
College of Technology

ACKNOWLEDGEMENTS

I would like to dedicate this work to my beloved family for their constant encouragement, support and unconditional love. I am deeply indebted to them.

I am grateful to my advisor, Dr. Alex Ignatiev, for giving me an opportunity to pursue Master's thesis under his esteemed guidance. I would like to thank him for providing me the opportunity to be a part of the Center for Advanced materials.

I would like to thank my supervisor, Dr. Nacer Badi, without whom this work would not be possible. I would like to extend my deepest gratitude to him for his invaluable suggestions, support and efforts in making this thesis possible.

My special thanks to Dr. Alex Freundlich and Dr. Francisco C Robles-Hernandez for accepting the invitation to serve on my thesis committee.

I would like to extend special gratitude to Dr. Ali Zomorrodian and Dr. Rabi Ibrahim for helping me in setting up the thermal evacuation chamber and carrying out XRD analysis and giving their valuable suggestions to improve my research activity.

Synthesis and characterization of scalable high permittivity core-shell ferroelectric polymers for energy storage solutions

An Abstract

of a

Thesis

Presented to

the Faculty of the Department of Electrical and Computer Engineering

University of Houston

In Partial Fulfillment

of the Requirements for the Degree of

Master of Science

in Electrical Engineering

by

Rakesh Mekala

December 2013

Abstract

Extensive interest is being invested into the research of polymer based nanodielectric films that provides a more practical energy storage solution primarily for embedded capacitors. Electrical dielectric constant (K) around 20 was reported using expensive gold (Au) coated with functionalized polystyrene (SiO_2) shell i.e.;(Au-SiO_2) nanoparticles inside a Polyvinylpyrrolidone (PVP) polymer matrix

This process has been improved as reported here by eliminating trivial functionalization steps to create a shell around a core by embedding a Polyvinilydine fluoride (PVDF) matrix, which is chemically inert to most solvents, with metal aluminum (Al) core nanoparticles surrounded by solid aluminum oxide (Al_2O_3) as a capping shell for electrical insulation.

Preliminary results show that proper loadings of oxidized aluminum (Al-Al_2O_3) nanoparticles in PVDF provide an improved dielectric constant and quality factor along with added structural flexibility. The dielectric constant, quality factor, frequency and thermal response of capacitance on structural parameters of the produced films for different loadings of embedded nanoparticles has been investigated. The effective dielectric constant of the nanocomposite has been modeled using COMSOL Multiphysics, and compared with experimental results. Also other dielectric properties of the nanocomposite have been studied using the simulation results.

TABLE OF CONTENTS

LIST OF FIGURES

LIST OF TABLES

CHAPTER 1: INTRODUCTION

1.1 Energy storage in electronic system

Energy storage is crucial in any electronic system starting from basic electronic devices to huge power systems which are used in industries. Capacitors that can store large amounts of energy and also deliver the stored energy instantaneously with high efficiency are highly desired in energy conversion systems, renewable energy storage systems along with many military and commercial applications like hybrid electric vehicle, electric aircraft, electric warships and so on [1].

Capacitors, supercapacitors and batteries can be classified with power and energy criteria. Capacitors carry higher power density with less energy density relative to batteries which have high energy and low power densities. Supercapacitors fall in between the capacitor and battery in terms of energy and power densities. To achieve high-energy storage along with instantaneous discharge of stored electrical energy combinations of the batteries and capacitors are used in some of the commercial applications like hybrid electric vehicles. Significant research is currently being carried out to increase energy storage capacity in a capacitor, which has a longer lifetime and can rapidly discharge the stored electrical energy [2], which if achieved can be considered as a super capacitor that can even replace batteries with further improvement in energy density. In printed circuit boards and many electronic devices passive components such as capacitors greatly limit the realization of higher energy systems as the size of the passive elements have to be greatly increased to store the required high energy. The ability of a capacitor to store energy depends on the dielectric material with which it is

made. So, engineering a new dielectric material meeting the above mentioned requirements could make a great foundation for future electronic systems.

1.2 Energy storage in capacitors

Capacitors are the dominating passive element in electronic systems that are used to store energy. Capacitors store static charge in a layer of insulating material sandwiched between conductive plates. A capacitor's size, dielectric constant and separation between the sandwiched plates determine the amount of energy it can store. Capacitors with high energy densities could make lighter electrical systems in case of hybrid vehicles, and cost effective energy conversion systems which can be extended to renewable energy resources [1]. With recent developments in technology and the need for miniaturization of the electronic components, capacitor area and separation between the metal plates have to be maintained low thus leaving the dielectric constant alone to be played around with to increase the energy storage capacity.

Electrical polarization is the principle used by dielectric materials to store electrical energy under an applied external electric field. Different kinds of electrical polarization are discussed in later sections. Along with polarization there is always some loss because of charge migration, which leads to conduction in dielectric material with dissipation of heat because of friction associated with molecular vibrations – this is called dielectric loss. The dielectric loss is required to be maintained well within permissible limits. Hence a dielectric material is expected to have high dielectric constant with minimal dielectric loss.

1.3 Energy storage issues in capacitor

It is difficult to achieve a dielectric material with high dielectric strength along with

high energy density. An attempt to increase one of the parameters has a great negative impact on the other. This is greatly seen in some of the commercial capacitors made with polypropylene, which can be operated at higher voltages meaning has high dielectric strength, but can relatively store only a small amount of charge in a given volume [3]. Ceramic capacitors are said to have high dielectric constant but they have inherent low breakdown field strength, which lowers the energy density of ceramic capacitor. Over years of research polymer-based nanodielectric material was considered to be the optimal solution to obtain high dielectric constant while maintaining good dielectric strength and dielectric loss under permissible limits. This polymer nanocomposite dielectric material takes the advantage of high dielectric strength of the polymer whose dielectric constant is improved by adding nanoparticles as fillers inside the polymer matrix. Thus by incorporating nanofillers into polymer composites both high dielectric strength and dielectric constant is obtained keeping dielectric loss in an acceptable range, which finally leads to higher energy storage [3].

1.4 Research Objective

The objective of this research is to produce a capacitor with a dielectric material made up of a polymer containing nanoparticles with the dielectric possessing high capacitance, high dielectric strength, high breakdown field, and low loss. The procedure used to develop such a dielectric material that is also cost effective the embedding of a Polyvinilydine fluoride (PVDF) matrix with high conductivity aluminum (Al) core particles having aluminum oxide (Al_2O_3) as a capping shell for electrical insulation. The primary goal of this work is to increase the effective dielectric constant of the composite formed by embedding Aluminum-Alumina ($Al@Al_2O_3$) core-shell nanoparticles in the

PVDF host matrix. Apart from increasing the dielectric constant, efforts have been made to maintain low dielectric loss, and to maintain considerable dielectric strength of the composite. Steps taken towards this include controlling the loading of nanoparticles in PVDF matrix, amount of PVDF used, and control of the processing techniques.

Effective dielectric properties of the prepared nanocomposites are also examined using COMSOL Multiphysics, which is a finite element method (FEM)-based simulation software that helps in predicting effective properties of the dielectric even before conducting an experiment. Earlier simulation work [4] indicated values, which were in high discrepancy with the experimental results because of consideration of highly ordered distribution of nanoparticles inside the polymer matrix. We propose to bridge this gap in the results by modeling nanodielectric films with less ordered nanoparticles in the polymer matrix so as to feedback the experimental work.

CHAPTER 2: BASICS OF A CAPACITOR

A capacitor is a two terminal electrical component to store energy electro statistically in an electric field. The forms of practical capacitors vary widely, but all contain at least two electrical conductors as electrodes separated by a dielectric insulator. When there is a potential difference between the electrodes an electric field is generated across the dielectric, causing a partial shift in positive charge to collect on the electrode at negative voltage, and negative charge to collect on the other electrode which is at a positive voltage. Energy is stored in the form of the electrostatic field. Although charges get accumulate on the plates of the capacitor there is no actual flow of charges inside it. An ideal capacitor is characterized by a single constant value capacitance denoted by C with charge Q stored on the electrodes and voltage V applied to the electrodes. Capacitance is given by the equation

$$Q = C^* V. \tag{1}$$

2.1 Capacitance

Capacitance is the amount of energy stored in a capacitor. The capacitance is a function of physical dimensions (geometry) of the conductors and the dielectric constant of the dielectric material used. Capacitance C is obtained from equation (1) given by

$$C = Q/V. \tag{2}$$

Capacitance is measured in farads (F), and its range varies from microfarad to pico farad. A ne-farad capacitor when charged with one-coulomb of electrical charge will have a potential difference of one-volt between its plates. Equation (3) shows that capacitance varies in direct proportion with area of the parallel conductors (A) and is

inversely proportional to the distance (d) between the conductors at which potential is applied.

$$C = (\varepsilon_0 * K * A)/d. \quad (3)$$

Where $\varepsilon = \varepsilon_0 * K$, represent the permittivity of the dielectric medium which is defined as the polarization capability of a given material when placed in an electric field; ε_0 is a constant known as permittivity of free space (8.854×10^{-12} F/m); K is dielectric constant.

2.2 Dielectric constant

The dielectric constant (K), also known as the relative permittivity of a material, is defined as the ratio of the amount of electrical energy stored in a material relative to that stored in a vacuum. In other words, it is a dimensionless quantity which is the ratio of permittivity of a medium to the permittivity of free space. Every material has its own dielectric constant. The dielectric constant for the vacuum is 1, and for all other materials it is greater than 1. Dielectric constant increases the capability of capacitor to store more charge as a capacitor filled with an insulating dielectric material can store K times more charge than an air dielectric capacitor with similar dimensions. In reality every dielectric material is associated with some loss and hence the dielectric constant is represented by a complex permittivity (ε) [4] with real (ε') and imaginary (ε'') parts given by:

$$\varepsilon = \varepsilon' + i * \varepsilon''. \quad (4)$$

The real part of ε is the dielectric permittivity, and the complex term signifies the dielectric loss of the material.

2.3 Dielectric loss

Dielectric loss seen in capacitors is a measure of their energy loss, which is due to the

movement of mobile charges inside the dielectric under the influence of an alternating field. Due to dielectric loss, the current to voltage angle deviates from ideal value of 90^0. This angular difference is termed the loss angle δ. This loss is also expressed in terms of the dissipation factor (DF) and quality factor (Q) which is represented by the following equation:

$$\text{Tan}(\delta) = DF = 1/Q. \tag{5}$$

The quality factor is also used to determine the quality of a capacitor. It is defined as the ratio of reactance to the resistive component in the circuit at a particular frequency. The higher the Q factor of the capacitor, the closer it approaches the behavior of an ideal lossless capacitor. Dissipation factors less than 0.1% are accepted. We generally want dielectric loss to be a minimum, thus a capacitor with low dissipation factor and high quality factor is the requirement.

2.4 Dielectric strength

The maximum electrical field strength that a material can withstand without loosing its insulating properties is termed its dielectric strength. An electric field applied above the dielectric strength value cause damage to the capacitor (breakdown), and this damage is permanent for all gaseous dielectrics [5]. Dielectric strength is expressed in units of volts or Kilovolts per unit of thickness. For a good dielectric material dielectric strength is always expected to be high which helps in operating at higher field strength.

2.5 Energy stored in a capacitor

The amount of energy (E) stored in a capacitor is expressed as follows:

$$E = \frac{1}{2} * C * V^2, \tag{6}$$

where V is voltage applied across the electrodes of capacitor. Hence, stored energy is directly proportional to the capacitance (C), which is related to the dielectric constant (K) of a capacitor. Thus, for high energy storage we need a high dielectric constant.

2.6 Dielectric Polarization

When an electric field is applied across a dielectric material it induces electrical dipoles inside the dielectric medium. This results in a slight change in position of positive and negative charge clouds under the influence of external electric field, which is termed as dielectric polarization. Dipoles orient in such a way that they create an internal electric field that opposes the applied field strength, thus reducing the effective field across the dielectric medium.

There are different types of dielectric polarizations, namely electronic polarization P_e, ionic polarization P_i, orientational polarization P_m , and space charge polarization P_s. Total polarization is sum of all these different polarizations. Electronic polarization (P_e) is the result of a relative shift of positive and negative charges in opposite directions within an insulator or dielectric induced by an electric field. Ionic polarization results from displacement of ions under an applied electric field, which results in dipole elongation. Orientational polarization is seen in materials with permanent dipoles created by unbalanced distribution of charge clouds. It is also known as dipole polarization. Space charge or interfacial polarization (P_s) occurs in composite systems where there is a significant difference in the properties of constituent materials. This mechanism takes place at the interface of the constituents and results in charge buildup.

CHAPTER 3: DIELECTRIC MATERIALS OVERVIEW

3.1 Organic polymers

Polymers that are not artificially synthesized and occur naturally are called organic polymers. Organic polymers show very high dielectric strength with good mechanical flexibility combined with low dielectric loss which greatly interest their application as dielectric materials, but they show very low dielectric constant if used alone as a dielectric material. There are two types of organic polymers, which are classified as polar and non-polar polymers.

Polar polymers have some permanent dipoles, which are created by an imbalance in the distribution of electrons, and in the presence of an electric field these dipoles will attempt to align with the applied electric field [6]. Movement of dipoles is associated with dielectric polarization, which depends on the frequency of the applied electric field. At very low frequencies dipoles have a longer time to get themselves aligned to the applied electric field, which greatly helps in increasing the dielectric constant of material. At very high frequencies dipoles find it difficult to align with fast varying field, which leads to lower dielectric constant.

The non-polar polymers on the other hand do not have any permanent dipoles because of symmetrical molecular structure, and thus dipolar polarization is absent in these materials. However, an applied electric field tends to move the electrons to create electron polarization which is of much lower magnitude as compared to dipole polarization, and thus non polar polymers have dielectric constants of value less than 3. Its magnitude has no dependency with frequency of applied field as electrons react instantaneously even at higher frequencies.

3.2 Ceramic dielectrics

Ceramic dielectrics, as the name signifies, are made of ceramic materials. They are the most widely used dielectrics due to their cost and efficiency. They are made from a variety of materials in many forms but the most commonly used materials are titanium dioxide, strontium titanate, and barium titanate [7]. Electronic Industries Alliance (EIA) categorizes ceramic capacitors into three classes namely Class-1, Class-2 and Class-3.

- Class-1 capacitors are the most stable of all ceramic capacitors in terms of operational temperature. They are usually use magnesium titanate or calcium titanate as the dielectric.
- Class-2 capacitors are less stable compared to Class-1 capacitors but they are more efficient volumetrically. Volumetric efficiency for a capacitor is one of the important figures of merit, and is the product of capacitance with the maximum voltage that can be applied to the capacitor. Class-2 are used as decoupling, by-pass and coupling capacitors, as efficiency is not an issue in such applications.
- Class-3 capacitors have high dielectric constant and high volumetric efficiency at room temperature. They are made with Barium titanate, which has a dielectric constant of up to 1250 [7], and are used as decoupling capacitors and for other power supply applications.

3.3 Thin film dielectrics

Thin film dielectric uses polymer or ceramic materials. Capacitors with such dielectrics typically have a cylindrical structure with two pieces of plastic film enclosed with metallic electrodes which acts as terminals. Usually thin film capacitors are not polarized, hence their electrodes are interchangeable. Thin film capacitors can be customized by choosing different film materials for the dielectric layer to get desired

characteristics like dielectric strength, stability and other electrical characteristics. Thin film capacitor values range from 100pF to few microfarads [7].

3.4 Dielectrics made from ferroelectric ceramics fillers in a polymer matrix

Polymers are basically electrical insulators with low dielectric constant and often high dielectric strength. On the other hand, ceramic fillers have high dielectric constant and thermal strength. Preparing a composite medium by combining two materials with different electrical properties might lead to a composite system that has superior electrical performance. Composites with native ceramics such as $BaTiO_3$, $BaSrTiO_3$, or $PbZrTiO_3$, which are embedded as fillers in a polymer matrix [1,3] have displayed K values of less than 100. However, K values of these composites were successfully increased to a value of 200 by modifying the intrinsic dielectric constant of the bare polymer. The major concern of ceramic/polymer composites; however is that they require very high ceramic loading, resulting in less mechanical flexibility and high dielectric loss due to lack of good dispersion of fillers in the polymer matrix.

3.5 Metal filled polymer composite dielectrics

Polymer composites embedded with metal particles were developed to increase the dielectric constant of polymer. It was observed that the electrical characteristics of such composites are close to the properties of metals but having all the mechanical properties of a polymer with processing method very similar to that used for polymer dielectrics [8]. The electrical characteristics of such a composite medium greatly depend on the amount of loading of metal particles, which is closely related to the percolation threshold. The concept of percolation threshold and percolation theory is explained with details in a later section. A high dielectric constant for the resulting composite medium can be obtained

with minimal loading provided that dielectric loss is maintained low by preventing the agglomeration of conductive metal fillers [9].

3.6 Nanodielectrics

Nanodielectric composites belong to a new type of materials that exhibit interesting physical, chemical, electrical and magnetic properties [5]. This is explained from the fact that metal nanomaterials are used as fillers replacing the conventional filler systems, thus forming nanocomposites. An important reason for this improved behavior is that nanoparticles have a higher surface interaction area than regular micron sized fillers. Another advantage of nanocomposites is their ability to attain higher capacitance densities with much thinner films. However, due to the tendency to form clusters of nanoparticles a conducting path is formed in the dielectric, which results in a catastrophic failure of the device. Therefore, uniform dispersion of nanoparticles is necessary to prevent these failures and to improve dielectric properties.

3.7 Core - shell hybrid filler polymer composite dielectrics

Direct contact of conductive fillers will result in a high dielectric loss because they form conduction path inside the dielectric. Therefore, a core-shell structure is proposed for nanofillers in which an insulating shell is coated around each conducting filler. These non-conductive shells act as inter-particle insulating barriers that prevent the conductive cores from coming in contact with each other. Core/shell structured nanoparticles can be synthesized using methods such as coating a non-conductive shell onto a conducting filler [10], oxidizing a conductive core to form a shell of its non-conductive oxide, which is observed in aluminum metal that forms alumina even when exposed to air. Core-shell

filler/polymer composites have high K values because of the increased net polarization of the dielectric and low tangent losses (δ) due to non-conductive shell.

CHAPTER 4: POLYVINILYDENE FLUORIDE POLYMER

Polyvinilydene fluoride (PVDF) is a semi crystalline polymer which possesses great ferroelectric properties besides its pyroelectric and piezoelectric properties. PVDF polymer is easy to process to get thin films. Some of its electrical characteristics such as high dielectric constant, relatively low dissipation factor and high dielectric strength have made this polymer useful as a capacitor dielectric material. Polymorphisms of PVDF exhibit crystalline structure in four phases:α, β, γ and δ. These phases give this polymer greater potential to exhibit diversity in dielectric behavior.

4.1 Advantages of Polyvinilydene fluoride polymer

PVDF is now being considered as a great candidate for polymer nanocomposites as it is highly non-reactive and resistant to solvents, acids, bases and heat, as well as low smoke generation during a fire event. PVDF has a low density (1.78) and low cost compared to the other fluoropolymers [11]. Apart from the above features, PVDF is highly ferroelectric which further enhances the dielectric response at lower electrical fields with a low loading of nanoparticles.

4.2 Different phases of polyvinilydene fluoride polymer

As noted, PVDF, exists in four different crystalline phases: α, β, γ and δ. It displays these diverse crystalline phases depending on crystallization conditions. The non-polar α phase is the common phase, which is obtained by a process called, melt crystallization at temperatures below 160^0C. The β-phase is the polar desirable phase due to its ferroelectric characteristics, and hence it is important to maximize β-phase in PVDF films used as dielectrics. The γ and δ are polar phases, but the magnitude of their dipole moment is much smaller compared to the β-phase. Thus, PVDF polymer containing β-

phase has garnered the most interest for electronic applications as it can provide the best ferroelectric properties. It is also possible to extract the β-phase from other phases by varying crystallization temperature and structural deformation [12].

It has been reported that PVDF films derived using N,N-Dimethylformamide (DMF) polar solvent have a polar β-phase [12], and they are used in the experimental procedure to prepare polymer and nanoparticle solutions. Extraction of different phases by varying the annealing conditions is explained in the later section.

4.3 Ferroelectricity

Ferroelectricity is the property of a material to show spontaneous polarization that can be reversed by an external electrical field. This mechanism of switching the polarization is accomplished by shifting the ions to opposite sides by an applied electric potential [13]. The so-called "order-disorder" materials belong to a special class of ferroelectric materials which are characterized by a transition from randomly oriented dipoles in the paraelectric phase to ordered dipoles in the ferroelectric phase. The paraelectric phase is the property of material that allows it to get polarized under external electric field even in the absence of permanent electric dipoles, unlike ferroelectrics that require permanent dipoles. Some of the dipolar ordering molecules including PVDF fall into this category of order-disorder materials. Hence, ferroelectricity plays a crucial role to improve K of a ferroelectric dielectric material.

4.3.1 Electrical polarization in polymer

Polymers exhibit three types of electric polarization [13], namely ferroelectricity, metastable dipolar dielectric orientation, and nonuniform space-charge distribution. These mechanisms are illustrated in Figure 1a-c. In the case of ferroelectricity (Figure

1a), the polarization occurs in the material with cooperative interactions that generate parallel alignment of permanent electric dipoles, which continue to remain in the equilibrium state [13]. The polarization in dipolar dielectric materials (Figure 1b), in contrast, is not as strong as in ferroelectrics as the alignment of the dipoles is primarily due to an applied external field with negligible or zero cooperative interaction among the dipoles. As a result the induced polarization is said to be in metastable state, and in the absence of an external electric field it will get back to its non-polar equilibrium state. In the case of non-uniform space-charge distribution (Figure 1c) trapped charge will produce an apparent polarization [13] which shows a non-zero magnitude even after the external field is removed. In case of the PVDF polymer, ferroelectricity is the dominant electrical polarization mechanism.

a)

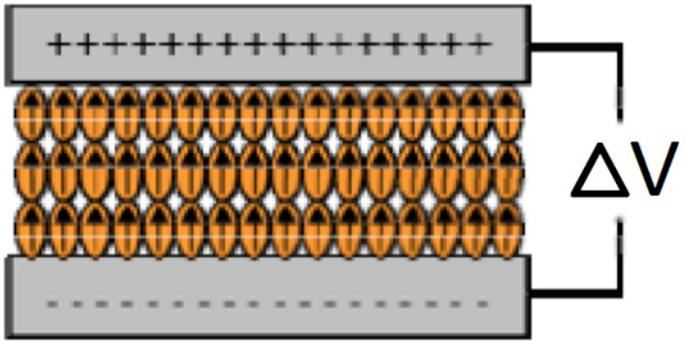

b)

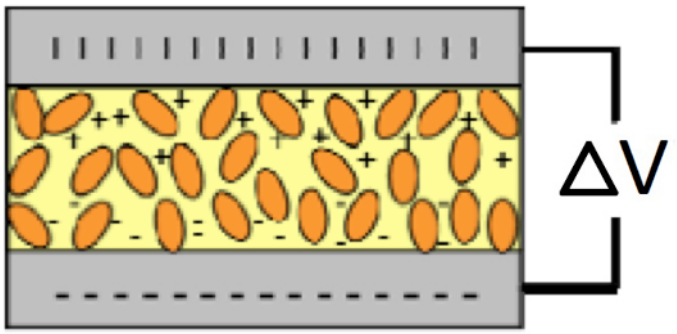

c)

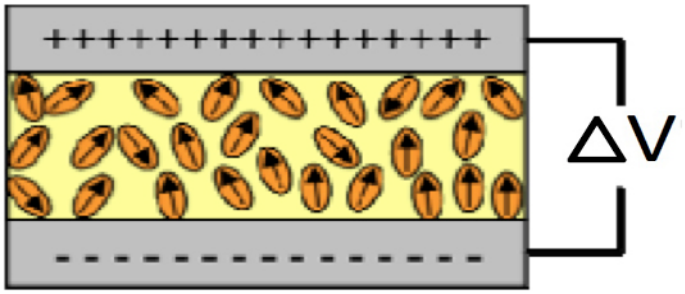

Figure 1. Manifestation of polarization in a) an ordered ferroelectric crystal, b) dipolar dielectric, and c) a space-charge dielectric material [13].

It is not usual to observe all three of the above mechanisms in semi-crystalline dipolar polymers. As a result, when attempting to characterize the ferroelectric properties of a given polymer system, care must be taken to insure that the polarization is truly bistable and that polarization reversal is indeed associated with the equilibrium properties of the medium and not external effects such as injected charge or metastable dipole alignment.

4.3.2 Ferroelectricity in polyvinilydene fluoride

PVDF stands out in ferroelectric behavior in β-phase because of its ideal molecular structure. The β-phase has an all trans planar zigzag structure as shown in Figure 2. In this all trans planar conformation dipole moments of the C-F and C-H bonds add up to yield an effective dipole moment in the direction perpendicular to the carbon backbone for every monomer. Hence, the β-phase has the largest spontaneous polarization thus exhibiting superior ferroelectric and piezoelectric properties. Ferroelectric behavior of PVDF is studied using simulated polarization values in the frequency range of 1Mhz – 10Ghz in section (7.2).

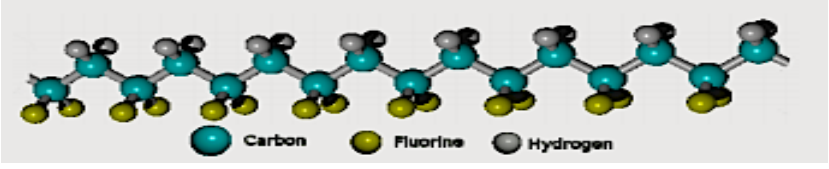

Figure 2. All-trans planar conformation of PVDF with a coplanar carbon back-bone [13].

CHAPTER5: EXPERIMENTAL PROCEDURE

5.1 Synthesis of polymer embedded nanoparticles

Preparation of samples by embedding nanoparticles into the polymer dielectric material involves a two-step fabrication process. The first step is to prepare an aluminum-alumina core-shell nanoparticle solution, and the second step is to mix the nanoparticle solution with the PVDF polymer solution, before spin coating the solution onto a Si wafer. Hereafter, aluminum-alumina core-shell nanoparticles will be denoted using the notation $Al@Al_2O_3$.

5.2 Aluminum nanoparticles

Aluminum nanoparticles used in the experiments are manufactured by American Elements Inc® [14]. The size of the aluminum nanoparticles used is calculated from the high resolution SEM images of fabricated nanodielectric composites and is found to vary between 60nm to 100nm in diameter. Precautions like use of masks to prevent inhalation of nanoparticles during experimental procedures must be used.

5.3 Preparation of polyvinilydene fluoride solution

As noted the aluminum nanoparticles are dissolved in DMF solvent, hence it is essential to choose a polymer that dissolves in DMF for the two solutions to be compatible, and PVDF readily dissolves in the DMF solvent which also gives us the feasibility to choose a particular phase of PVDF by simply varying the curing temperature as explained in section 4.2. The DMF - PVDF polymer solution is placed in a beaker, covered with a parafilm and aluminum foil to prevent evaporation of solution, and is stirred in a thermolyne stirrer for 3 hours.

5.4 Preparation of the Aluminum-Alumina ($Al@Al_2O_3$) solution

Aluminum nanoparticles when exposed to air form an Al_2O_3 shell because of the highly reactive nature of aluminum. This eliminates the need of a functionalization procedure to form an insulating shell around the metal aluminum core. The $Al@Al_2O_3$ core-shell nanoparticles are mixed into a DMF polar solvent which facilitates the use of polar mechanisms like dielectric polarization. This solution is taken in a beaker covered with parafilm and aluminum foil to prevent evaporation of solution, and is sonicated in a high-power Mesonic sonicator to break-up any agglomerates for 120 min with the solution maintained at room temperature.

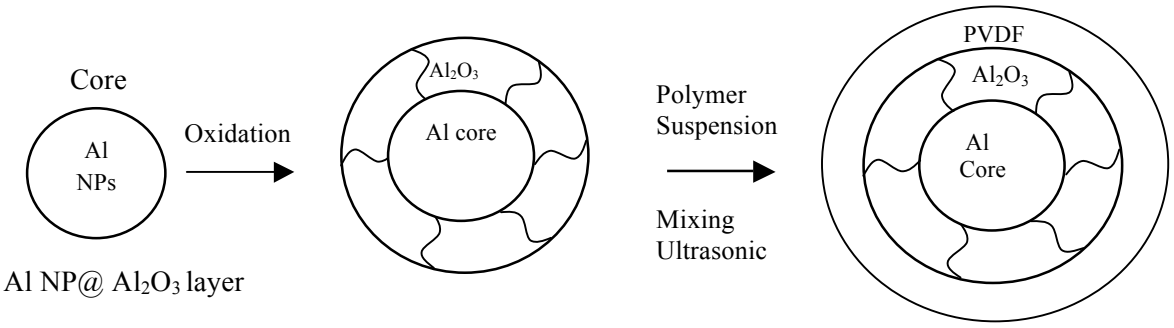

Figure 3. Illustration of the proposed fabrication steps of Al-Al_2O_3/PVDF core-shell nanodielectric.

5.5 Mixing polymer and nanoparticle solution

The $Al@Al_2O_3$ nanoparticle DMF solution is mixed with the PVDF dielectric, and is then is fabricated into a thin film by spinning the solution onto a substrate. The important step in determining the characteristics of the nanodielectric is mixing the PVDF and $Al@Al_2O_3$ nanoparticle-DMF solutions in proper proportions as the capacitance of the film coated using $Al@Al_2O_3$ nanoparticles and PVDF depends on the concentration of nanoparticles (also termed as loading) in the dielectric.

PVDF and nanoparticles solutions are sonicated thoroughly for 3 hours before mixing them. After mixing the individual solutions in required proportions, the mixture is thoroughly sonicated before it is spin coated onto the substrate. This ensures dispersion of nanoparticles in the polymer matrix with proper blending in the final solution.

5.6 Si Wafer Cleaning Procedure

The PVDF and $Al@Al_2O_3$ solution mixture is spin coated onto a Si wafer, which acts as base for fabricating capacitors. Before spinning the solution mixture, the Si wafer is cleaned to removed grease and surface dust. Trichloroethylene, acetone and methanol are used in similar volumes to clean the wafer. 10ml of each of these solvents are put into a beaker with the Si wafer. This is sonicated in an ultrasound sonicator bath for one minute with the substrate then dried on a hotplate at 120^0C for 1min. To ensure the removal of any oxide layer on the wafer, it is rinsed in a solution containing a 1:10 ratio by volume of Hydrofluoric acid (HF) and water. Finally, the wafer is blown with dry nitrogen gas after rinsing with Milli Q water.

5.7 Spin Coating the Nanodielectric

After cleaning the Si wafer, it is cleaved into pieces and again blown with nitrogen gas before mounting it on a spinner. A Spinner is a platform which is capable of spinning a substrate like Si wafer. When a solution is dripped onto the wafer before or during spinning, a thin film is formed on the substrate. The thickness and uniformity of the film depends on the solution's viscosity and the spinning pattern followed. For thin films, higher spinning speed is used with a less viscous solution and vice versa for thicker films. A small amount of the PVDF and $Al@Al_2O_3$ solution mixture is placed on the Si wafer using a pipette. Before placing the solution, the Si wafer is centered on the spinner and is

held in its position using vacuum, which completes the pre-spinning setup. Now the spinning pattern has to be determined which is crucial at this stage. A sequence of trial and error attempts was made to find the best spinning procedure that would lead to a 1-step spinning process. This process, which is used to fabricate all the dielectric samples mentioned in this work, entails a spinning at a speed of 1000rpm speed for 12 min at which time the dielectric is spin coated on the substrate and is ready for post-processing.

5.8 Post-Processing the Nanodielectric

Post-processing is one of the key stages in fabrication as it plays an important role in deciding the material characteristics of the dielectric. Post-processing a PVDF dielectric increases its breakdown strength and decreases the dielectric loss. This post-processing involves heating the spin-coated dielectric to a temperature that allows PVDF to crosslink. As a part of this work, curing temperatures over a range of 30^0C to 120^0C were tested for 10 minutes on each sample. From the results it was determined that samples which were cured at 120^0C for 10 minutes showed β and γ phases in the polymer of which β-phase has highest ferroelectric nature as explained earlier. As a result, this curing process is used with all the samples associated with this work.

5.9 Top electrode deposition

The spin coated and cured dielectric is now ready for top electrode deposition which involves physical vapor deposition of a metal film in a vacuum chamber. When a top electrode is coated, the fabricated device completes the structure of a parallel plate capacitor with a metal top electrode, a Al@Al_2O_3/PVDF nanodielectric layer in the middle, and a Si wafer at the bottom acting as a bottom electrode.

5.9.1 Physical Vapor Deposition

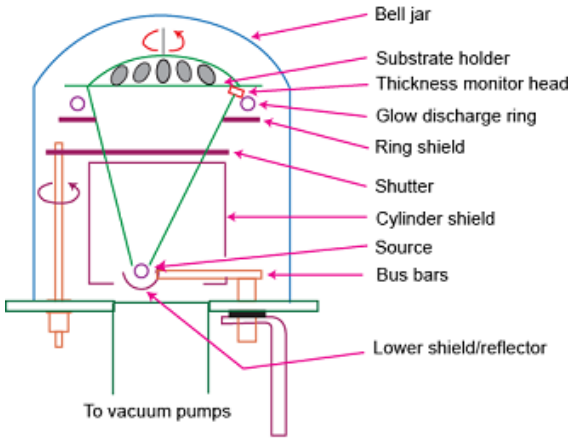

Figure 4. Schematic of Physical vapor deposition evaporation [27].

The thermal evaporation technique is a physical vapor deposition technique which requires high temperature to melt the source material into the vapor state. The atoms or molecules of the source material are accelerated by high temperature allowing them to pass through the vacuum space and deposit onto substrate surface. A vacuum environment is required to reduce contamination of the evaporated film by background gases and to allow free motion of the evaporating atoms/molecules in the chamber. As represented in the schematic shown in Figure 4, the source contains an alumina coated boat crucible which holds the source material and is heated by a heater supported by the bus bars connected to a high current power supply. The substrate is held above the source on a substrate holder, and a shutter blocks the deposition of source material onto the substrate until it is opened for deposition. Thickness of the source material deposited onto the substrate depends on the deposition rate of vaporized material and duration for which shutter is opened. Figure 5 below shows the actual physical vapor deposition chamber setup which was used in the experiments carried out.

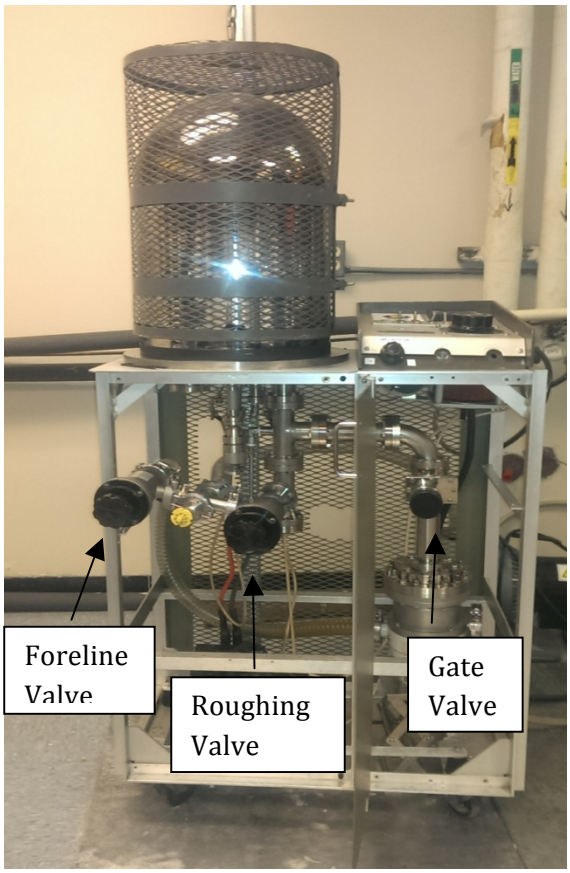

Figure 5. Physical Vapor Deposition chamber.

Figure 5 shows the deposition chamber with a foreline valve, a roughing valve to separate chamber form mechanical pump, and a gate valve to isolate turbo pump from the chamber. The main chamber is connected to a turbo pump, which maintains the base pressure of the chamber at 10^{-6} Torr. A chiller circulates cold water around the turbo pump in a loop to dissipate the generated heat. The substrate is first loaded into the substrate holder with source material loaded into source inside the chamber. The chamber is first pumped with a dry rotary mechanical vacuum pump. After the chamber pressure reaches a value of 10^{-3} Torr, the gate valve is opened which brings down the chamber pressure to 10^{-6} Torr by the turbo pump.

5.9.2 Stencil Mask Design

Before the nanodielectric coated Si wafer is placed in the vacuum chamber for deposition it is masked with a stencil mask to make metal deposition of desired shapes and sizes. A thin aluminum plate stencil mask with a square hole 3mm on a side is used for the deposition of Al top electrode. Therefore, all the devices in this research are parallel plate capacitors with 3mm square metal films as the top electrode. Figure 6 shows a schematic of the aluminum mask used. Other designs of stencil mask can also be used to make devices of different shapes and sizes on the same Si wafer.

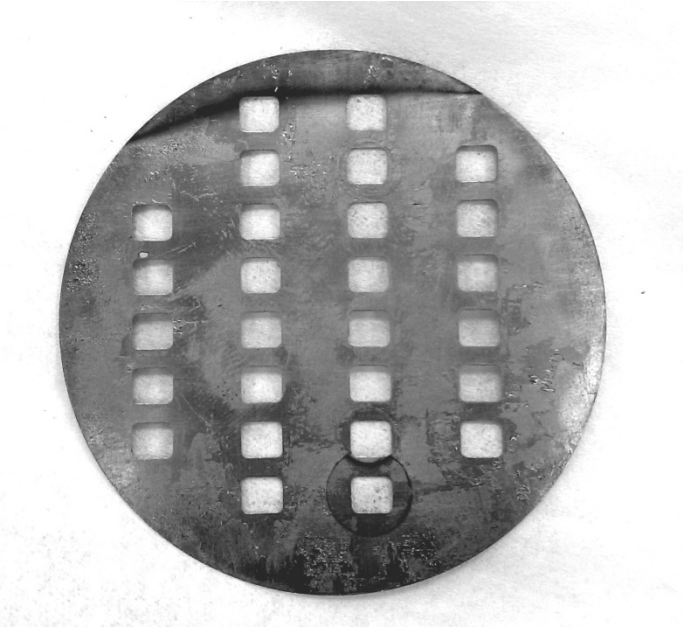

Figure 6. Stencil mask with square opening of side 3mm.

5.9.3 Physical vapor Deposition process:

After masking the substrate with the stencil mask it is loaded into the chamber and the chamber pumped as described in the section 5.9.1. Before the mechanical pump is turned on, chilled water line is turned on to prevent damage of turbo pump. The deposition process involves turning on power to the source boat once the chamber is at the required

deposition pressure. A quartz crystal thickness monitor is used to read the deposition rate of source material. The thickness monitor is placed beside the substrate. When the shutter is opened, the substrate gets deposited by the source material and thickness monitor starts displaying the deposition rate at (Å/s). Deposition takes place at below 10^{-5} Torr pressure, and is continued until the required thickness is obtained on substrate after which the shutter is closed and current through crucible is slowly brought down to 0 amp. The experimental developmental steps in making the capacitor device using synthesized nanodielectrics are shown in Figure 7.

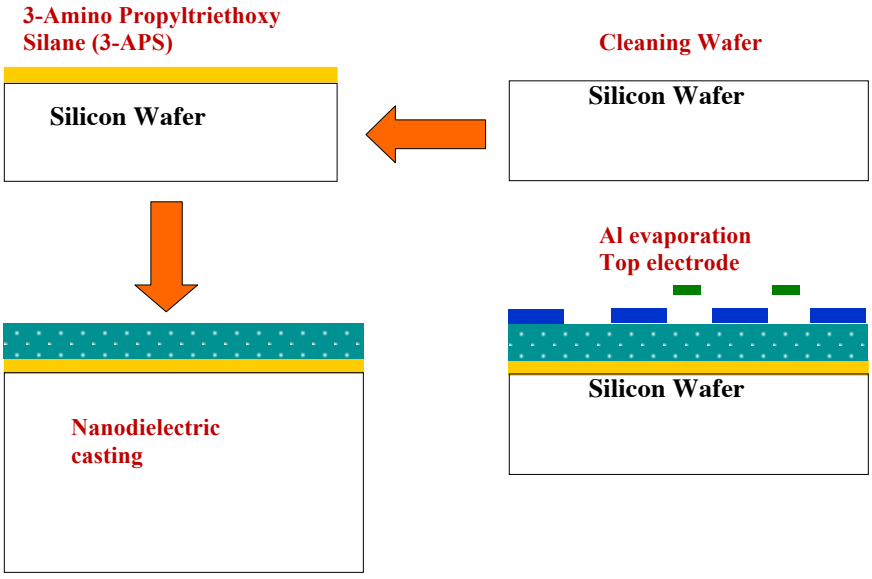

Figure 7. Fabrication steps in making planar capacitor devices.

CHAPTER 6: COMSOL Multiphysics simulation

The effective dielectric properties of the nanocomposites are modeled using COMSOL Multiphysics, a finite element method (FEM) based simulation software. FEM analysis is generally used to decrease the development times and predict the output patterns for a variety of processes. This saves time and expensive production costs. The primary goal of simulation in this research is to calculate the effective dielectric constant of the composite medium formed by PVDF and $Al@Al_2O_3$ core-shell nanoparticles and to study the polarization and electric field dependence on fraction of loading. Polarization dependence on frequency is also studied so as to study the ferroelectric property of PVDF material. An in-plane AC model was used in COMSOL multiphysics software to simulate the effective properties of nanofillers embedded in polymer dielectric composite capacitors.

6.1 FEM SIMULATION

The finite element method (FEM) also known as finite element analysis (FEA) is a quantitative technique used to find approximate solutions for partial differential and integral equations. FEM requires a problem to be defined as a geometry, which is subdivided into a number of symmetrical identities called mesh elements. The complex dielectric function of PVDF is calculated using the Drude theory. The effective dielectric constant of the composite dielectric medium can be calculated by using percolation theory and generalized effective medium theories (EMT) [17]. Percolation theory helps in determining the behavior of the composite system near the percolation threshold using a simple power law expression, which is described in later sections.

6.2 Background theory

6.2.1 Drude theory for dielectric material

Debye [15] considered a set of dipoles free to rotate in opposite direction of the applied electric field to determine relaxation of polarization in a dielectric material with a single relaxation time. The equation for complex permittivity proposed by Debye is as follows:

$$\varepsilon^* = \varepsilon_\infty + \frac{\varepsilon_0 - \varepsilon_\infty}{1 + i\omega\tau} \tag{7}$$

Where ε_0 = Dielectric constant at low frequency,

ε_{00}= Dielectric constant at high frequency,

ω= Angular frequency, and

τ= Relaxation time.

According to Frohlich, the real and imaginary parts of the dielectric permittivity are given by

$$\varepsilon'' = \frac{\varepsilon_0 - \varepsilon_\infty}{1 + i\omega\tau}(\omega\tau) \tag{8}$$

ε' , the real part, determines the permittivity of a material in the presence of an electric field, and ε'' the imaginary part, determines the intrinsic loss mechanisms involved in the dielectric medium.

6.2.2 Dielectric function of core-shell nanoparticle

A core-shell hybrid filler configuration is proposed to reduce the dielectric loss associated when metal nanoparticles alone were used as fillers [15]. An insulating shell is formed around each metal nanoparticle, which helps in configuring metal-insulator core-shell type particles. It is important to calculate the dielectric permittivity of the particles

themselves to measure the effective dielectric constant of a composite made with core-shell nanoparticles. The effective dielectric permittivity of core-shell nanoparticles is given by following equation

$$\varepsilon_{cs} = \varepsilon_c * \left(\frac{1 + (a * [\varepsilon_c - \varepsilon_s])}{\varepsilon_s + (b * [\varepsilon_c - \varepsilon_s])} \right) . \quad (9)$$

where ε_{cs} is the dielectric function of the core-shell particle, ε_c is the dielectric function of the metallic core, ε_s is the dielectric constant of the shell material, a is analogous to area fraction of core which is given as $(r_1/r_2)^3$ for 3D particles, and b is a depolarization factor with value 1/3 for spheres (3D). The radius of the core is given by r_1 and that of the shell is given by r_2.

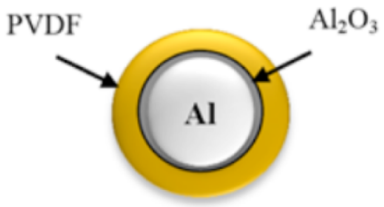

Figure 8: Model of Nano-Metal polymer composite.

6.2.3 Effective Medium Theory

Effective medium theories (EMT) and other mean-field like theories are physical models based on properties of individual components and their fractions in the composite structure [16]. Generally, the properties that are calculated using EMTs are the dielectric constant and the conductivity. There are many EMTs, and the accuracy of each theory is dependent upon different conditions. Most popular EMTs [17, 19] are as follows:

the Maxwell – Garnett model,

$$\varepsilon_{eff} = \frac{1}{4}\left[3f(\varepsilon_i - \varepsilon_h) + 2\varepsilon_h - \varepsilon_i + \sqrt{(1-3f^2)\varepsilon_i^2 + 2(2+9f-9f^2)\varepsilon_i\varepsilon_h + (3f-2)^2} \right] \quad (10)$$

and the Symmetric Bruggeman model,

$$\varepsilon_{eff} = \varepsilon_h + 3f\left(\frac{\varepsilon_i - \varepsilon_h}{\varepsilon_i + 2\varepsilon_h}\right)\varepsilon_h \qquad (11)$$

where ε_{eff} is the effective dielectric constant of the medium, f is the volume fraction of the filler, ε_i is the dielectric constant of the Al filler, and ε_h is the dielectric constant of the host PVDF matrix.

6.2.4 Percolation theory

The technique to increase dielectric constant of polymer based capacitors by preparing percolative composites greatly depends on the concentration of the nanofillers. As mentioned earlier, when loading of the nanofillers is in the vicinity of the percolation threshold the effective dielectric constant of the composites can be increased dramatically. In percolation theory distribution of fillers in the composite medium depends on the filler shape, size and orientation, and is independent of materialistic properties of the fillers or host medium [20]. Percolation theory is significant when loading of fillers reaches a critical value called the percolation threshold (f_c). At this threshold value substantial changes take place in the physical and electrical properties of the system. Using COMSOL multiphysics variation of dielectric constant is studied using percolation theory. The abrupt difference in the properties of aluminum (electrical conductivity) and PVDF (electrical conductivity) gives us a good platform for use of the percolation theory. A simple power law relation, equation (13), can be used to describe the changes in the system properties near the percolation threshold as

$$K * K_h = |f - f_c|^{-s} . \qquad (12)$$

Where K is the effective dielectric constant, K_h is the dielectric constant of the host PVDF material, f is a fraction of the inclusions, f_c is the fraction of inclusions at the

percolation threshold, and s is an exponent of value 1.

6.3 Use of COMSOL Multiphysics

Simulation in COMSOL can be broadly classified into three steps: creating geometry, setting the model and solving the model.

6.3.1 Creating the geometry

Creating a geometry that is most suitable to the problem being solved is the first step in the COMSOL simulation. The geometries needed for simulation of the composite nanodielectric environment are drawn in 3D models with varying filler fractions. Each loading fraction in either model is created as a separate file with an independent geometry. Figure 9 shows the geometry setup of the 3D model for the nanodielectric embedded core-shell nanoparticles with spherical disks of core diameter 35nm and shell diameter 45nm that are enclosed in a cubical block of size 350nm that defines the PVDF polymer matrix. The locations of the different nanoparticles are randomly generated by a MATLAB function, and the corresponding geometry is built in COMSOL software helping the simulation results to be more appropriate to the experimental results.

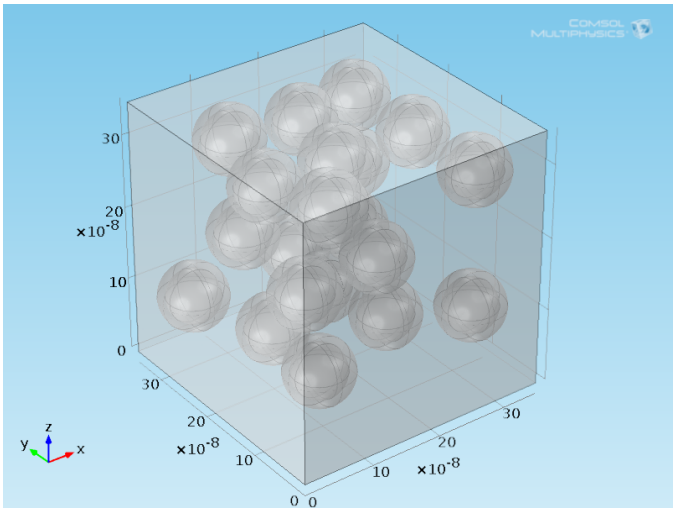

Figure 9. Polymer matrix with randomly dispersed nanoparticles.

6.3.2 Setting the model

In COMSOL Multiphysics, the electrostatics in-plane electric current module was used to simulate the effective properties of $Al@Al_2O_3$ core-shell nanofiller/PVDF composite capacitors. This module allows a frequency sweep to be conducted for different loadings of the nanofiller at different frequencies. In sub-domain settings, the polarization (P) of the composite determined by equation (13) is chosen as the basic governing equation as it is the major concept of the governing physics of metal-insulator composite nanodielectric capacitors.

$$P=\varepsilon_0*(\varepsilon_r-1)*E \quad (13)$$

where E is the electric field, ε_0 represent the permittivity of free space and ε_r represent the permittivity of dielectric medium of composite material. After completion of the geometry, sub-domain settings are used to assign materials to the different sections of the geometry. In a 3D geometry, the top face is set to the input the positive potential where input-alternating voltage (sine function is considered in simulations with unit amplitude) is applied while maintaining opposite the face at ground. The remaining sides are maintained as periodic boundary condition. This gives the geometry that is analogous to a parallel-plate capacitor with a voltage applied across its plates.

6.3.3 Solving the model

The final steps before simulating the model is declaring the physical properties and defining the guiding equations and constants with corresponding variables. There is also a privilege in COMSOL to do the parametric sweep for selected parameters. In the following simulations frequency of the input sinusoidal voltage was varied and the corresponding characterizations are studied and plotted, which completes the model building that can be analyzed and solved.

CHAPTER 7: RESULTS

After fabrication of a capacitor as described in chapter 6, it was characterized to determine the device performance. The dielectric constant, quality factor and thermal response are considered to characterize the fabricated capacitor. Also XRD and SEM analysis was done to understand the structural composition of the prepared composites. The dielectric constant of PVDF is calculated for a range of frequencies using Drude theory. The effective dielectric constant of the composite is calculated using Effective medium theories and percolation theory as mentioned in section 6.2.4. Results from COMSOL Multiphysics simulated 3D models for varying filler concentrations are analyzed and compared.

7.1 Fabrication Results

7.1.1 Producing uniform PVDF Film

It is important to understand and optimize the technique for fabricating polymer films which display the best possible characteristics of Al@Al_2O_3/PVDF composite films. Initially, films were made exclusively with PVDF to understand its functioning as a dielectric matrix. Thin PVDF films were made using the procedure mentioned in Chapter 4. To optimize the procedure for use of PVDF as an efficient dielectric, experiments were conducted with different concentration of PVDF solutions, varying spinning patterns, and a range of curing temperatures. Table 1 lists procedures involved in making the PVDF samples and their results.

Table 1: Polyvinilydene fluoride film uniformity test at varying concentration and curing temperature.

Sample no	Amount of PVDF	Spinning pattern	Curing temperature	Film thickness	Result
1a	1gm	10s at 100rpm, 10s at 500rpm, 20s at 2000rpm and 30s at 3000rpm	130^0C	1.8μm	Substrate breakage
2a	1.5gm	10s at 100rpm, 10s at 500rpm, 20s at 2000rpm and 30s at 3000rpm	120^0C	2.5μm	Substrate breakage
3a	2gm	10s at 100rpm, 10s at 500rpm, 20s at 2000rpm and 30s at 3000rpm	110^0C	3.3μm	Substrate breakage
4a	2.5gm	10s at 100rpm, 10s at 500rpm, 20s at 2000rpm and 30s at 3000rpm	57^0C to 80^0C At 80^0C for 10 min 80^0C to 100^0C and at 100^0C (10 min) 100^0C to 120^0C at 120^0C (10 min)	4.2μm	Substrate breakage

The amount of polymer listed in Table 1 was mixed with 13ml of N,N-Dimethylformamide (DMF) solvent and mixed thoroughly using a magnetic stirrer to form a clear solution. A small amount of mixture, approximately 0.2ml, was used to make thin PVDF films on quarter of a 2-inch silicon wafer (Si) using a Laurell Technologies WS-400 spinner followed by curing on a hotplate. Before spin coating acleaned Si wafers it is spin coated with 3-Aminopropyl triethoxy silane to improve the adherence of deposited film dielectric film onto the Si wafer [21].

3mm square Al top electrodes were deposited by PVD with the help of a stencil mask. The thickness of the prepared dielectric films was measured using scanning electron microscopy (SEM). The PVDF concentration used for sample 3a gave a film with considerable thickness which is standardized for proceeding samples in the experiment, but the film obtained was non-uniform and substrate breakage occurred for all the samples. The reason for this was considered to be the spinning pattern and curing procedure. Based on reference [3], the spinning patterns shown in Table 2 are considered.

For the spinning patterns listed in Table2 that of sample 2b was to be used for succeeding samples; however, the curing procedure needed to be improved to prevent the irregularities obtained on the surface of film. Curing in vacuum for 12hours at defined temperature with pre-curing at 90^0C for 10min greatly improved the samples with reduction of irregularities on prepared film. To test the repeatability of this technique, multiple samples were made with the same recipe and all of them showed the same characteristics. Hence, spinning patterns of 1000rpm for 12 min and pre-curing temperature of 90^0C is standardized for proceeding samples.

Table 2: Polyvinilydene fluoride film uniformity test at varying spinning pattern.

Sample no	Amount of PVDF	Spinning pattern	Curing temperature for 10min	Film thickness	Result
1b	2.5gm	800rpm for 12min	90 ^{o}C	4.8μm	Improvement in uniformity of film but with irregularities
2b	2.5gm	1000rpm for 12min	90 ^{o}C	3.6μm	Improvement in uniformity of film but with irregularities
3b	2gm	1200rpm for 12min	90 ^{o}C	2.5μm	Improvement in uniformity of film but with irregularities
4b	2.5gm	1500rpm for 12min	90 ^{o}C	1.6μm	Improvement in uniformity of film but with irregularities

7.1.2 Phase of PVDF

As described earlier in section 4.2, the phase of the PVDF material in prepared film depends on curing temperature, and hence the different phases of PVDF were studied by varying the curing temperature. Table 3 lists the various phases obtained for the different curing temperature with varying spinning pattern.

Table 3: Phases of Polyvinilydene fluoride.

Sample	700rpm	1000rpm	1500rpm	2000rpm	30^0C	90^0C	120^0C	160^0C	Phase
1	√				√				α,γ
2	√					√			β
3	√						√		γ,β
4	√							√	γ
5		√			√				α,γ
6		√				√			β
7		√					√		γ,β
8		√						√	γ
9			√		√				α,γ
10			√			√			β
11			√				√		γ,β
12			√					√	γ
13				√	√				α,γ
14				√		√			β
15				√			√		γ,β
16				√				√	γ

Hence, to get high dielectric constant the beta phase is preferred, which needs a curing temperature around 90^0C. However, curing at this temperature leaves some irregularities on the fabricated film, hence, a curing temperature of 120^0C is preferred, which also yields the β-phase along with some γ-phase and gives a uniform dielectric film. Therefore, the procedure mentioned in section 7.1.1 with a post curing temperature of 120^0C, was used as a standard on all the samples discussed further in this work. From the above samples, the dielectric constant (K) for PVDF was established as 12 and is in agreement with the results published by other research groups [22]. This dielectric constant value of PVDF is used throughout the rest of this work.

7.1.3 Characteristics of Al@Al_2O_3/PVDF Films

The successful optimization of the technique to fabricate PVDF as a dielectric led to an advancement of polymer dielectric films fabricated with embedded Al@Al_2O_3 core-shell nanoparticles. A capacitor using unloaded PVDF as a reference sample and two capacitors with different volume loadings of Al@Al_2O_3 fillers in the PVDF host polymer were fabricated. The capacitor devices were then characterized for their capacitance characteristics using an HP-4275A high frequency LCR meter. Table 4 represents the specifications of the fabricated capacitors such as quality factor, capacitance as well as the average value characteristics of tested capacitors at 10 KHz. The dielectric constant of fabricated capacitors can be calculated using the measured capacitance, the thickness of dielectric, and the area of the electrodes (area of the 3mm square electrode) from Table 4 and equation (3).

Table 4: Characterization of fabricated capacitors

	Tested Capacitors		
	1	2	3
Capacitance (pF)	262	250	300
Thickness (nm)	3600	5500	6340
Quality factor	100	160	730
Loading (Vol. %)	0	10	20
Dielectric constant (K)	12	17.3	23.6

The dielectric constant of the bare PVDF is calculated to be 12. This increases to a value of 17.3 with a nanoparticle loading of 10% by volume. With further addition of nanoparticles the dielectric constant value is doubled when loading reached 20%by volume. The quality factor increased with increasing loading of Al nanoparticles in the insulating polymer, which is most likely due to the good electrical contact between the top aluminum electrode and polymer nanocomposite. Figure 10 shows the frequency behavior of typical capacitors with 3mm x 3mm square Al top electrode. Each reading of the capacitance represents the average value of measurements taken on an array of 5 capacitor units. For comparison purpose, the capacitance values are normalized to the same film thickness of 6340 nm. The electrical characterization shows reproducible and stable capacitors over frequencies up to 10 MHz.

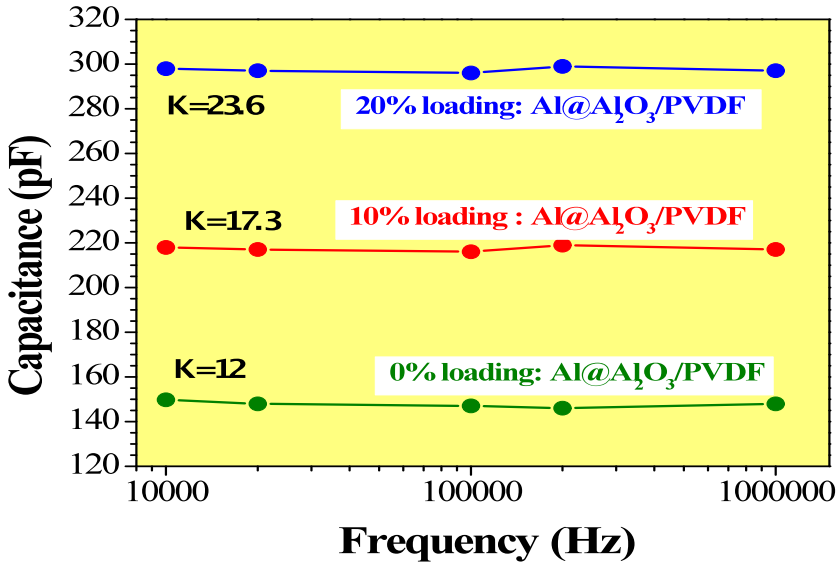

Figure10. Dependence of capacitance on frequency for tested capacitors ranging from 150 pF to 300 pF as normalized to the same film thickness of 6300 nm.

Figure 11 describes the thermal characteristics of the fabricated capacitors. Capacitors were heated on an ALESSI-4500 THERMOCHUCK test bench from room temperature to melting point of PVDF polymer i.e.; 170^0C. The capacitance was calculated using an HP-4275A LCR meter for capacitors with pure PVDF as dielectric and with loading of 10% and 20% by volume of nanoparticles. It is observed that capacitance showed steady response until the temperature reached the pre melting point of 70^0C, and decayed thereafter. However, the capacitor with high loading (20%) of nanoparticles showed a drastic fall in capacitance when the temperature reached 70^0C. This might be due to high loading and also to the polymer being thermally less conductive compared to that of the aluminum nanoparticles, which leads to a decay of the interfacial interaction between the polymer and the nanoparticles with increase in temperature. Under these conditions the nanoparticles are no longer bonded by the polymer matrix which gives rise to high dielectric loss and decay in dielectric constant. This phenomenon was observed to be

reversible i.e., capacitors retrieved their original capacitance value when temperature was brought down to room temperature.

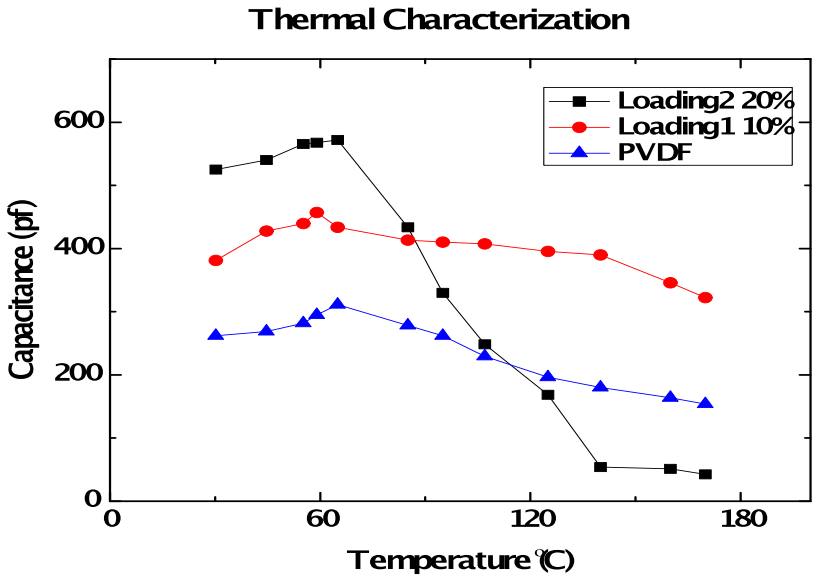

Figure 11. Thermal characterization of fabricated capacitors.

7.1.4 Structural Analysis

In nanodielectrics, agglomeration of nanoparticles is the major reason for many device failures. Local spots with increased electric field concentration are created, known as hot-spots, due to agglomeration. The presence of hot-spots creates an imbalances in the charge distribution, which results in electron conduction through the dielectric leading to catastrophic failure of the device [20]. This can be prevented by uniform dispersion of nanoparticles in the dielectric.

To study the arrangement of nanoparticles laterally, SEM analysis was conducted using an FEI XL-30FEG on the cross-section of the Al@Al_2O_3/PVDF nanodielectric with the data shown in Figure 12. The high resolution SEM picture in Figure 13 shows the

particle size of core-shell nanoparticles embedded in the PVDF matrix. The size of nanoparticles ranges from 60 – 100 nm and the Al2O3 shell is about 15 nm.

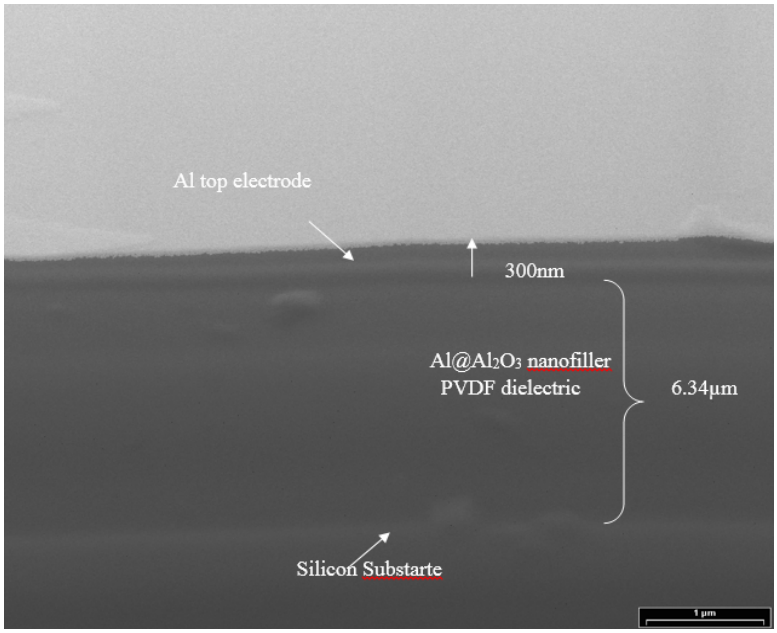

Figure12. SEM pictures of parallel-plate capacitor cross-section.

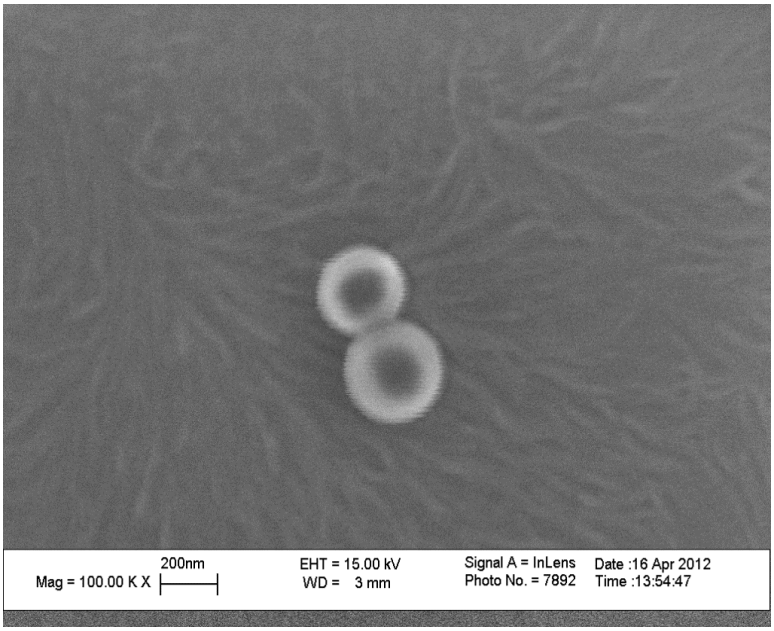

Figure 13. SEM images of $Al@Al_2O_3$ NPs in the PVDF matrix.

X-ray diffraction analysis was carried out for prepared nanodielectric to look for the phase of PVDF polymer, and to measure the aluminum and alumina materials. The XRD peaks in Figure 14 positioned at diffraction angle (2θ) of 20.1^0 and 20.3^0 confirm [12] the presence of the γ (110), and the β (200,110) phases of PVDF. Also the XRD peak at 38.52^0, 44.67^0, 65.13^0, 78.27^0, 28.56^0, 26.64^0, 34.67^0 identify the presence of Al (111), Al (200), Al (220), Al (211) [23], Si (111) [25], α-Al_2O_3 (012), and α-Al_2O_3 (104) [24] respectively.

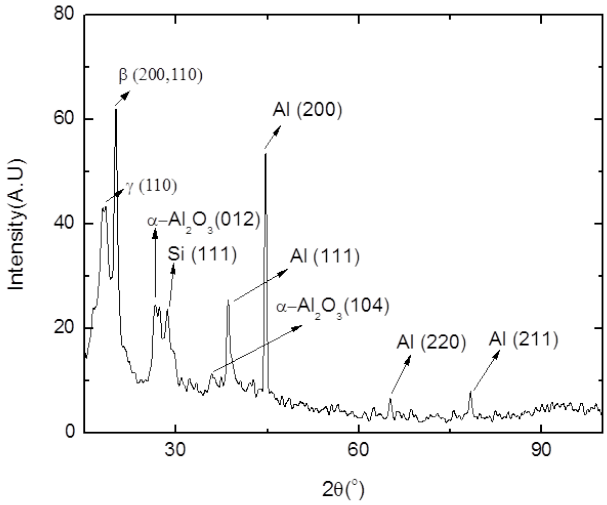

Figure 14. XRD image of Al@Al_2O_3 NPs in PVDF matrix.

7.2 FEM SIMULATIONS

7.2.1 Dielectric constant of PVDF

The complex dielectric permittivity of the PVDF material is calculated by Drude theory for dielectric material to calculate its complex dielectric function using equation [8] considering the damping term to be (logΓ= -16.41) and a dielectric constant (ξ_0) of 12 at low frequency and a dielectric constant at higher frequencies (ξ_{00}) approximated to be 4.5.

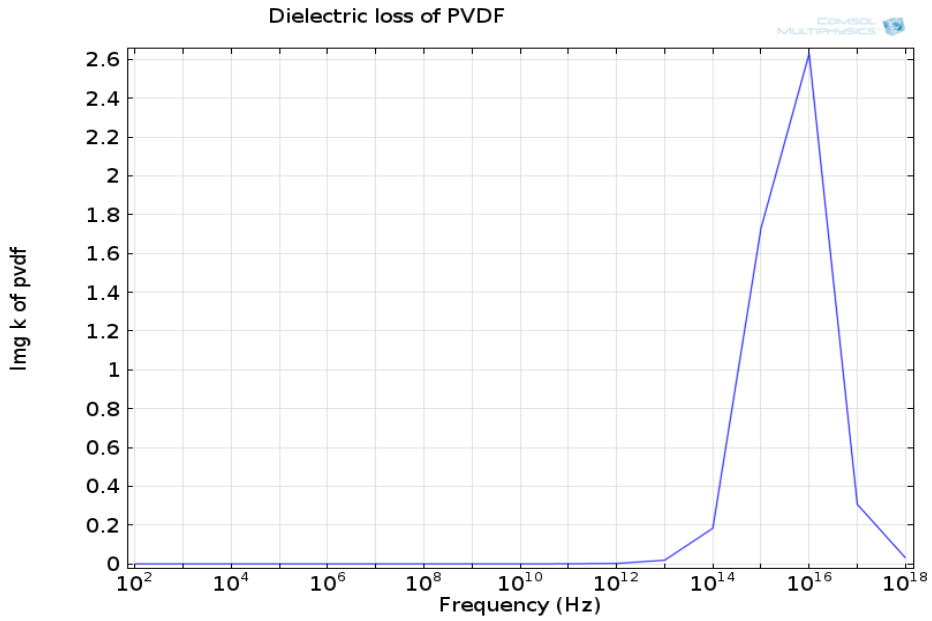

Figure 15. Imaginary part of dielectric function of PVDF.

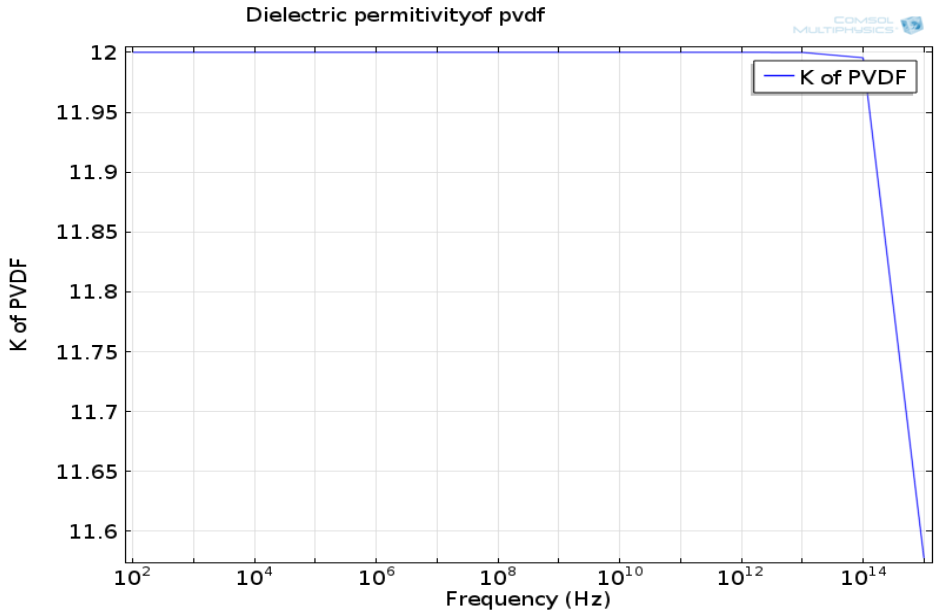

Figure 16. Real part of dielectric function of PVDF.

Figures 15 and 16 describe the complex dielectric permittivity behavior of PVDF with frequency using equation (8). The real part of dielectric function, which is the dielectric permittivity of PVDF remained constant until a frequency of 10E13Hz is

reached, and there after it decays with increase in frequency due to increased dielectric loss (imaginary part of dielectric function) in the frequency range of 10E13Hz to 10E16Hz.

7.2.2 3D Modeling

When a voltage is applied across the dielectric, an electric field is generated in the direction shown in Figure 17a. When nanoparticles are embedded in the PVDF matrix, an additional electric field ($E_{Polarization}$) is generated in the opposite direction due to the orientation of surface charges of the nanoparticle fillers, as shown in Figure 17b. This leads to a decrease in effective electric field ($E_{effective}$) inside of the dielectric as per equation (14), along with increase in the polarization of dielectric medium as the embedded nanoparticles polarize and orient in the direction of effective electric field. According to equation (15), the dielectric constant (K*)* of the composite should increase when $E_{effective}$ decreases with a resultant increase in polarization.

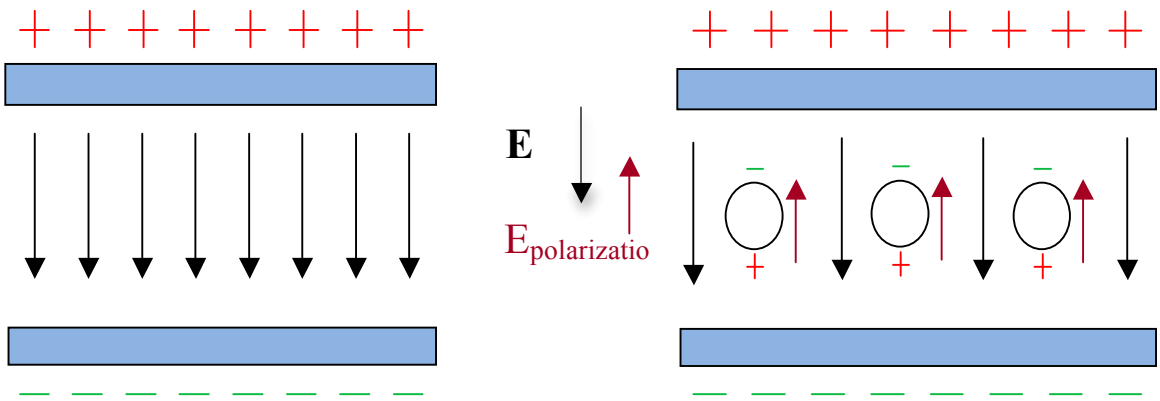

Figure 17: Electric field in (a) pure PVDF dielectric (b) Al@Al2O_3/PVDF nanodielectric.

$$E_{effective}=E-E_{Polarization} \quad \text{and} \tag{14}$$

$$P=\varepsilon_0(K-1)E_{effective} \tag{15}$$

Generation of electric field and polarization due to the introduction of nanoparticle fillers is studied using COMSOL Multiphysics simulations. Built-in functions available in the COMSOL multiphysics software are used to calculate the electric field and polarization distribution inside of the dielectric medium. In 3D simulation, cases with different loadings of $Al@Al_2O_3$ core-shell nanoparticles were considered, with the results compared to the bare PVDF polymer. Figure 18 shows the modeled electric field distribution in the composite nanodielectric medium with nanoparticle loading fraction varying from 0 to 0.12. It was observed that as the loading increased the effective electric field in the composite dielectric medium decreased from $2.69*10^6$(V/m) in the case of pure a PVDF medium, to $1.12*10^6$(V/m) for a loading fraction of 0.12. This is because the internal electric field, namely $E_{polarization}$, increased from a null value in case of a pure PVDF medium to a value of $1.57*10^6$(V/m) for a loading fraction of 0.12 thus following equation (14).

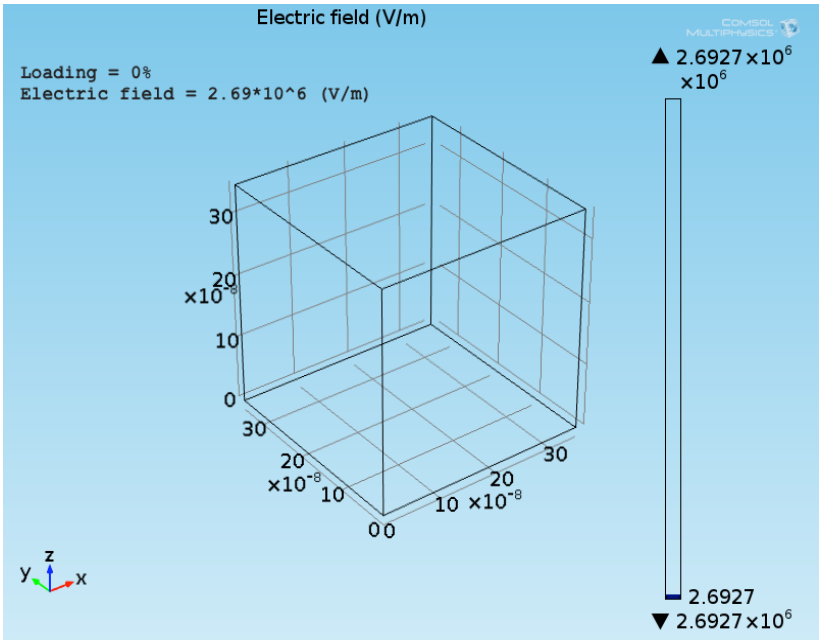

(a)

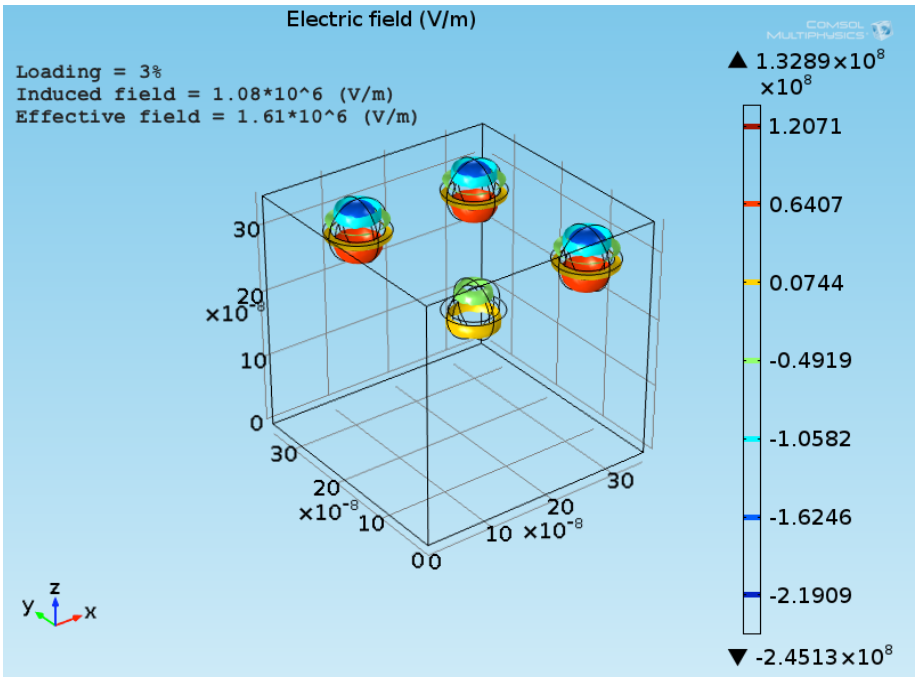

(b)

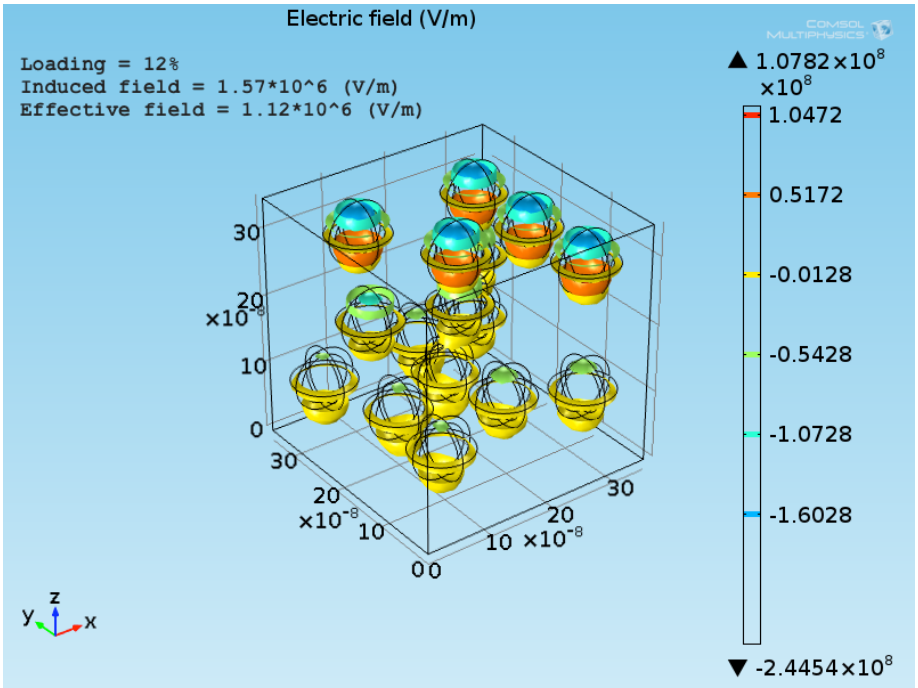

(c)

Figure 18. Electric field in 3D nanodielectric with loading of (a) f=0, (b) f=0.03 and (c) f=0.12.

Color tables to the right in the Figure 18 are used to identifiy the electric field value across the dielectric medium. It can also be inferred using the color table that field reversal takes place at every nanoparticle with red color signifying the maximum electric field, which is observed at the bottom surface of nanoparticle and blue color for the field observed at top surface of the nanoparticle. Thus, the effective field across the nanoparticle i.e., $E_{polarization}$ is opposing the applied electric field resulting in reduction of the effective electric field in the medium. It was also observed that closer the nanoparticle is to the positive electrode the greater is the field across the nanoparticle.

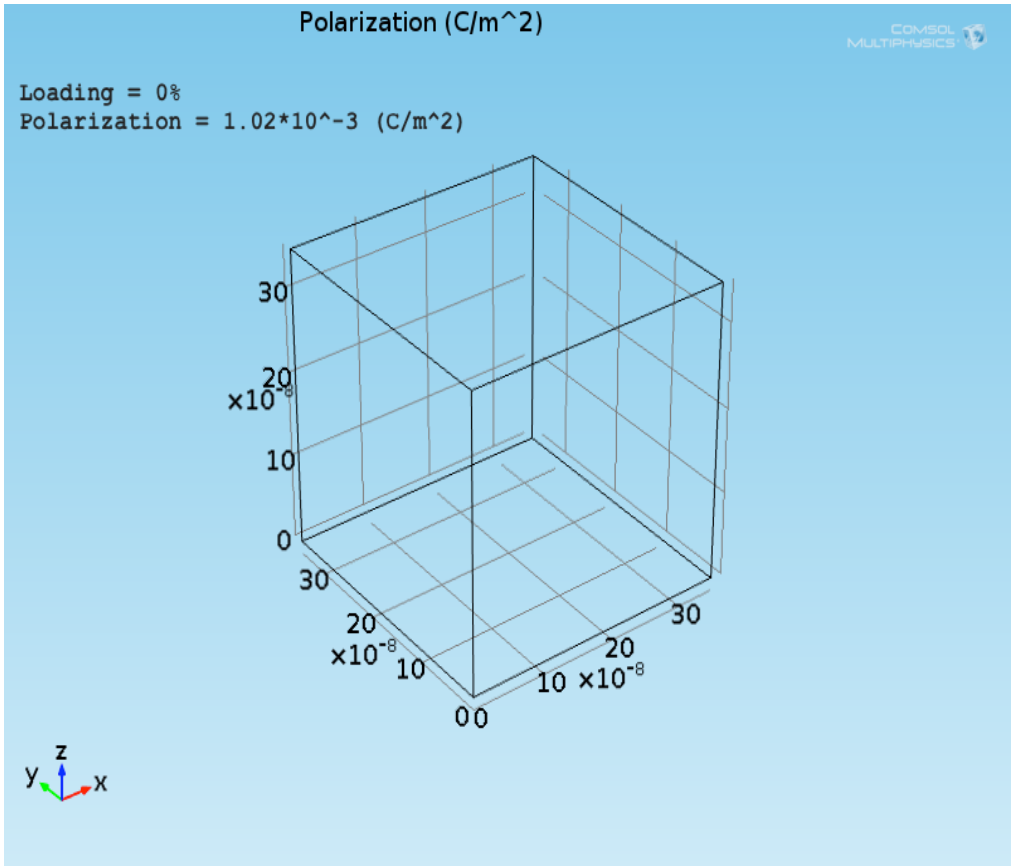

(a)

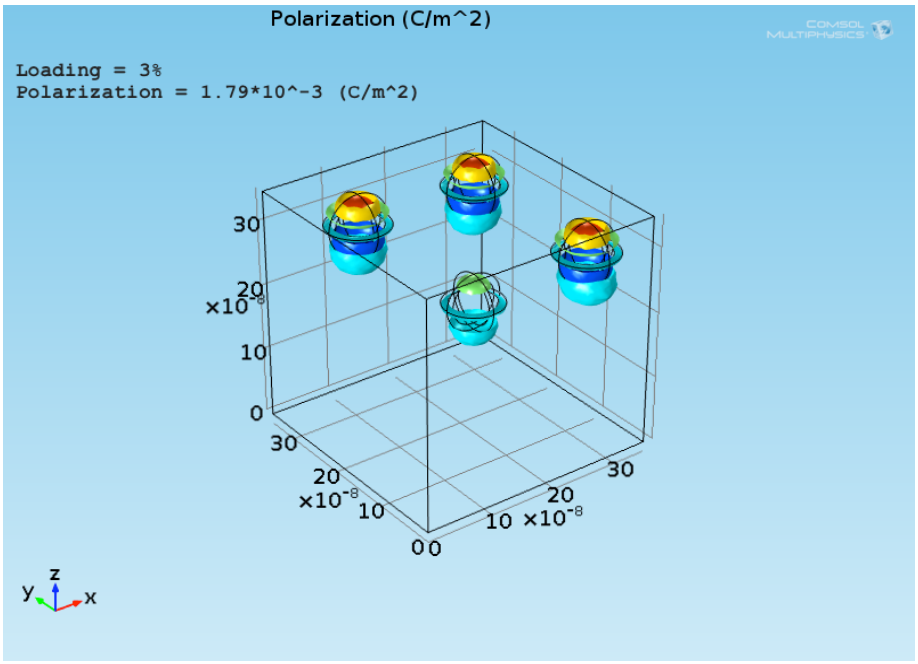

(b)

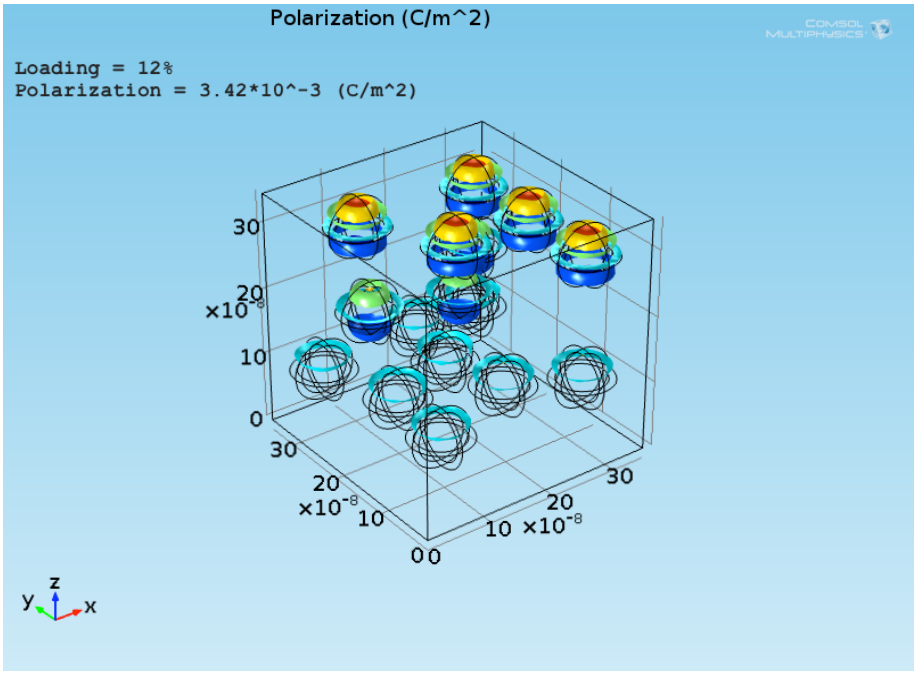

(c)

Figure 19. Electric polarization in 3D nanodielectric with loading of (a) f=0, (b) f=0.03 and (c) f=0.12.

Similarly Figure 19 shows the polarization plot for the dielectric medium composite with nanoparticle loading fraction varying from 0 to 0.12. It was observed from the figure that as the loading increased, polarization of the composite medium was found to increase from a value of $1.02*10^{-3}C/m^2$ for a pure PVDF medium to $3.42*10^{-3}C/m^2$ for the medium with loading fraction of 0.12. This points to the fact that the addition of nano sized fillers into the polymer matrix helps to increase the net polarization of the medium with reduction of the effective electric field around the composite dielectric medium. Thus from equation (15) the dielectric constant of the composite dielectric medium should increase with increased loading of fillers, which is shown by the percolation theory plot in Figure 20.

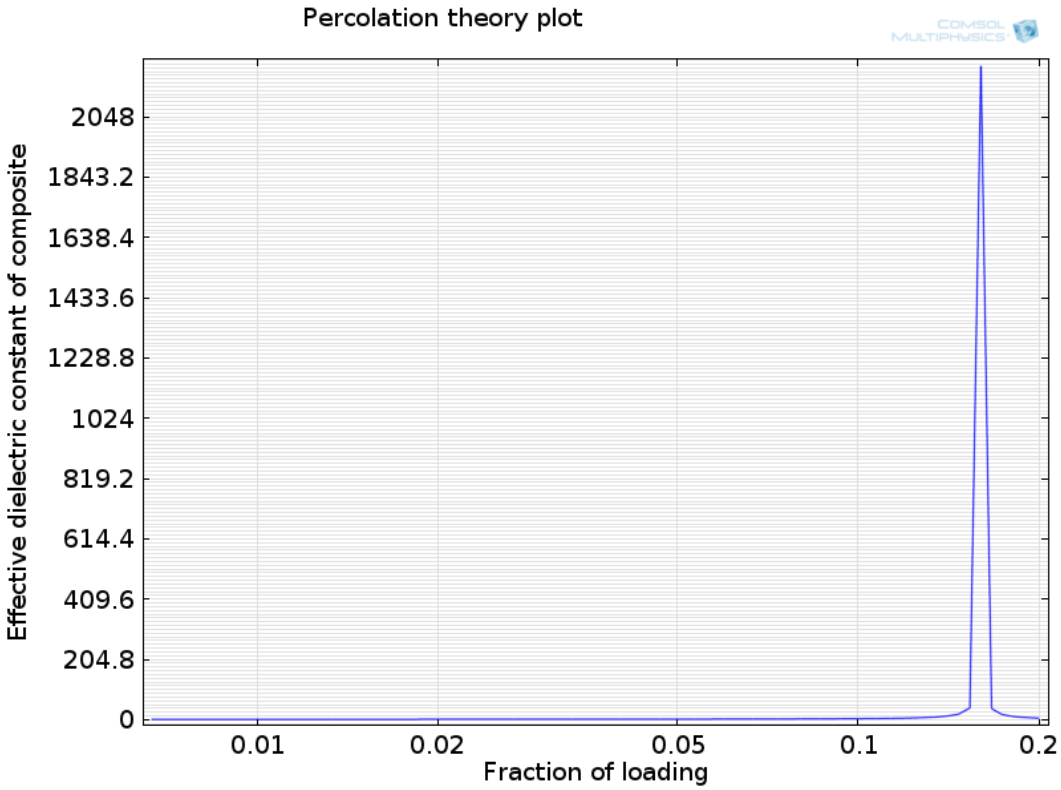

Figure 20. Percolation threshold plot.

In the percolation theory plot in Figure 20 it is observed that with increased loading the dielectric constant increases until the percolation threshold loading of 0.16 where dielectric constant has a value of 2800. Beyond this loading the dielectric constant drastically until the fraction of loading attains a value of unity. This is because the dielectric will no longer have its insulating properties, and starts behaving like a conductor beyond the percolation threshold. According to percolation theory the dielectric constant should decay after the percolation threshold loading of 0.16, but it was observed in the experimental results that the dielectric constant further increased from 12 to 23.6 when the loading fraction increased from 0 to 0.20, which is beyond the percolation threshold. This is because Percolation theory doesn't consider the materialistic properties and inter-particle interactions of the nanoparticles involved in the medium but depends only on the fraction of fillers, size of fillers used and dielectric constant of host polymer matrix. Figure 21 shows the percolation plot of the dielectric constant from 0 to 0.14 loading

Percolation theory calculated dielectric constant of bare polymer to be 12 which increased to a value of 39.02 at a loading fraction of 0.10. Obtained results were in good agreement with experiment results which were found to be 12 and 17.3 for the bare polymer and the polymer with loading fraction of 0.10. As it is practically difficult to achieve the percolation threshold loading fraction of 0.16, the region of interest for the modeling work was near to the percolation threshold loading to achieve high dielectric constant.

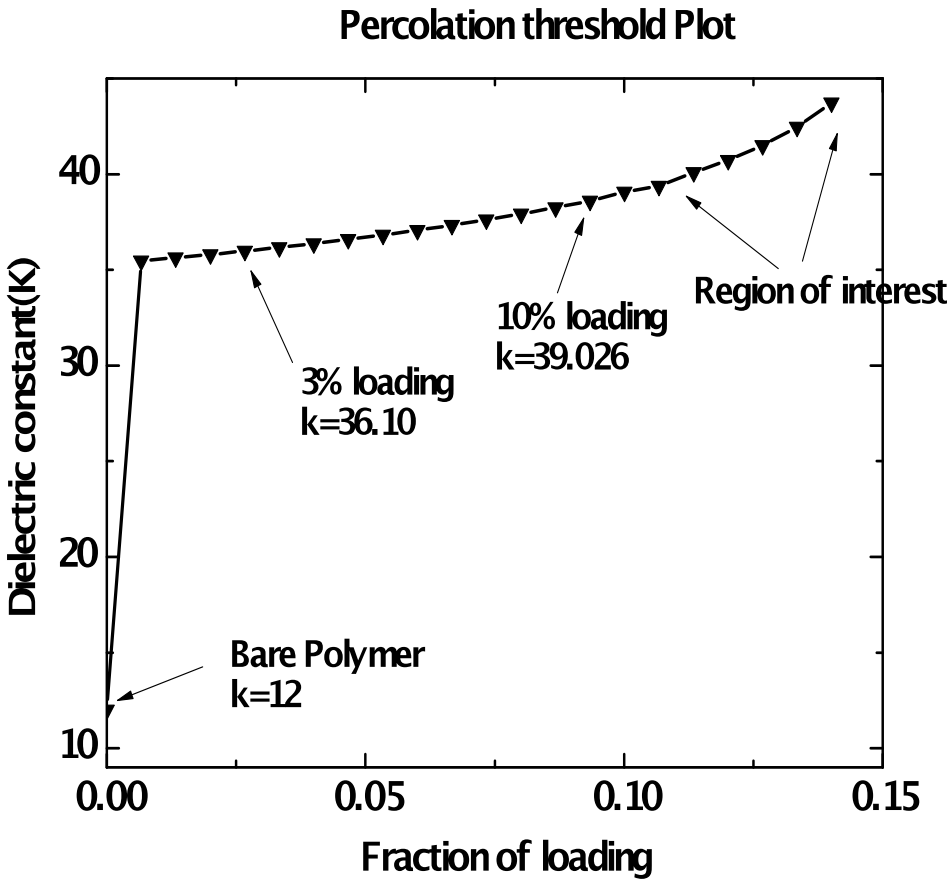

Figure 21. Percolation threshold plot with fraction of loading varying from 0 to 0.14.

7.2.3 Dielectric constant calculation using Effective Medium Theories

The dielectric constant of the medium is also calculated using the effective medium theory equations (10) and (11) for loading fraction of 0.20 by varying frequency from 10Hz to 10E15Hz. The dielectric constants of aluminum (1.6) and alumina (9.4) are used to calculate the composite dielectric constant of the core-shell structure using equation (9).

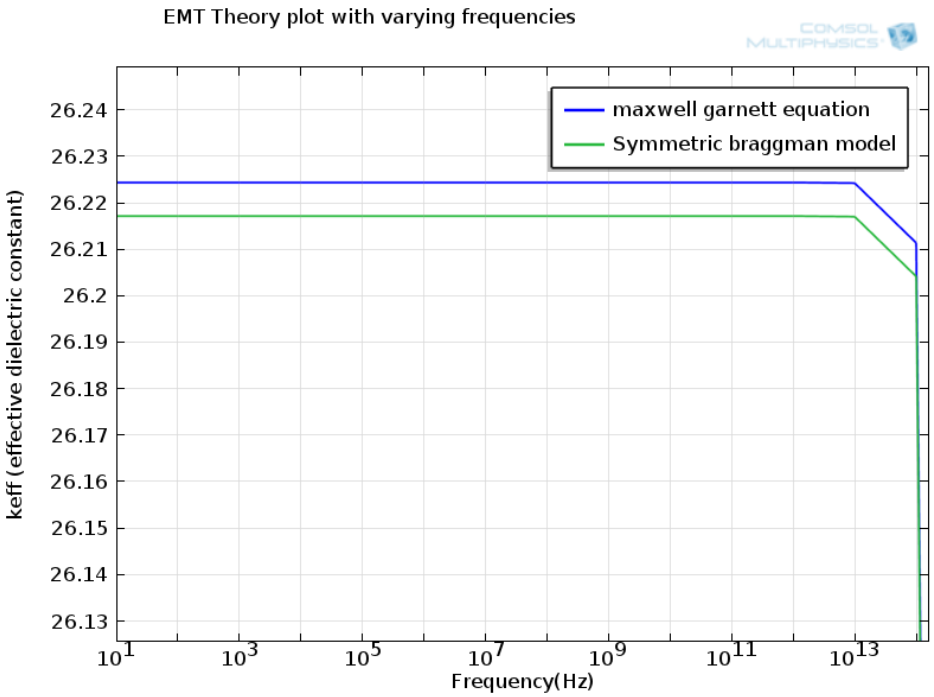

Figure 22. EMT theory plot of dielectric constant with varying frequency calculated for polymer embedded with 10% loading of $Al@Al_2O_3$ nanoparticles by volume.

It is seen from Figure 22 that the calculated K value remained constant until a frequency of 10E12Hz, and there after decayed with increase in frequency. This is because only atomic and electronic polarization mechanism are observed at frequencies greater than 10E12Hz, both of which are of much lesser magnitude than the other polarization mechanisms. The calculated K value of 26.2 using EMT showed close match with the experimental results of 23.6 at a loading fraction of 0.20. The experimental results also showed response relatively constant value of K in the frequency range of 10Hz to 1Mhz.

7.2.4 Case study at the interaction of two shells

The interaction of two Alumina shells was studied to understand the electrical insulation produced by the alumina shells when two core-shell nanoparticles are in close contact to each other. Simulation results clearly showed that polarization dropped from

16.83E-5 C/m^2 at the shell to 5.62E-5 C/m^2 at the interaction surface. This clearly signifies how non-conductive alumina shells act as inter-particle barriers and prevent the conductive cores from coming in contact with each other.

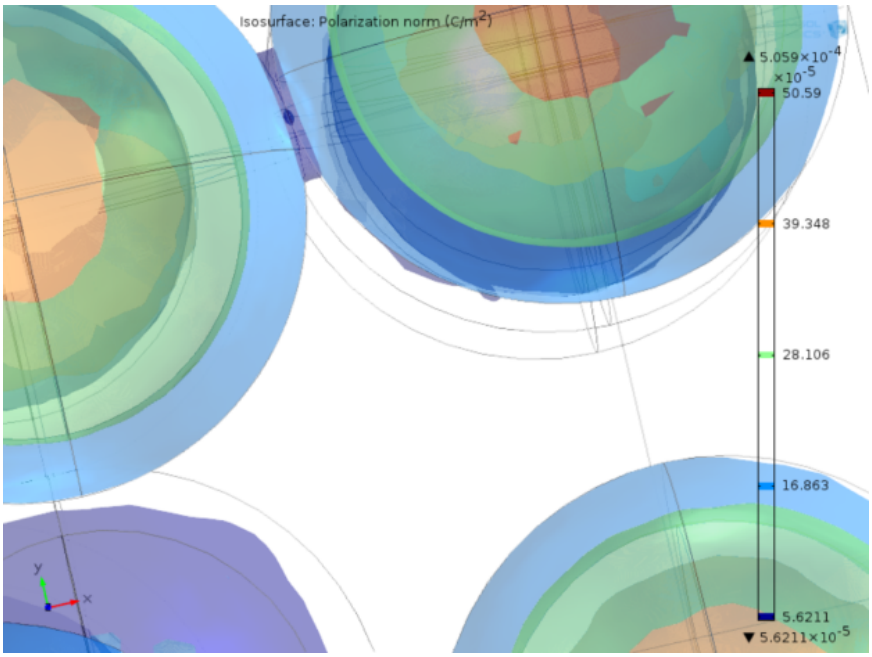

Figure 23. Polarization plot at the interaction of alumina shells.

Figure 24 illustrate the electric field orientation in pure PVDF polymer and polymer embedded with nanoparticles when an electric potential is applied. Arrows with length proportional to the magnitude proportional to the field represent field orientation. As explained earlier, the electric field deviates near surface of the nanoparticles with the particles bending in a direction to oppose the applied electric field. The higher the loading the greater is the field reversal across the nanoparticle, which further reduces the effective electric field around the composite dielectric medium.

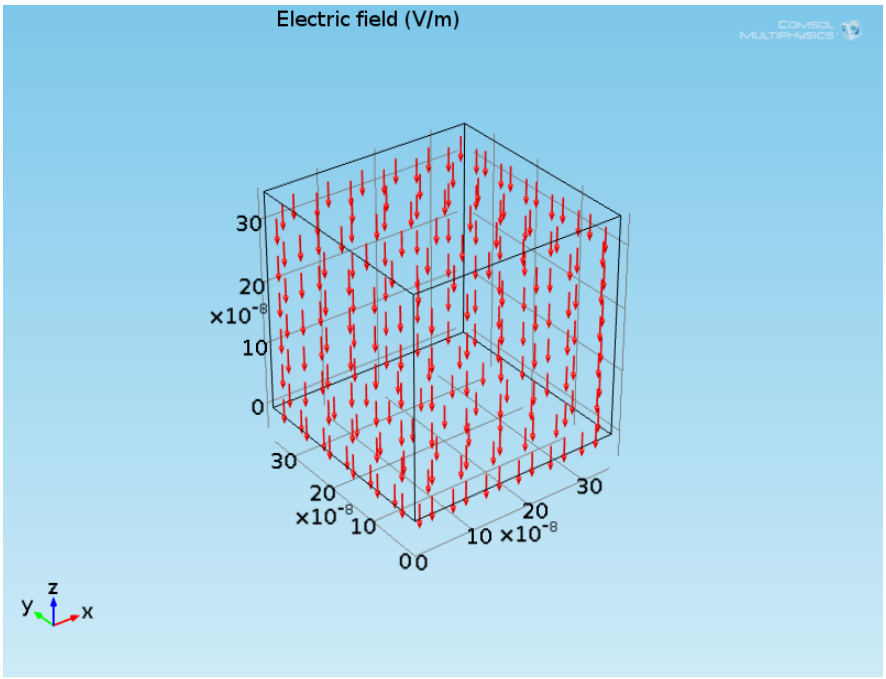

(a)

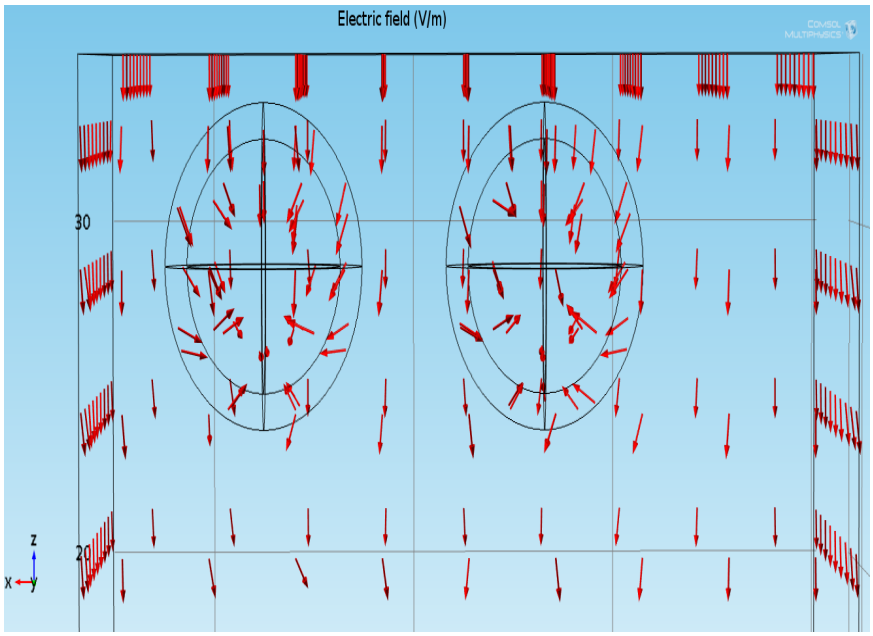

(b)

Figure 24. Electric field orientation in a) PVDF polymer b) PVDF polymer embedded with nanoparticles.

7.2.5 Polarization plot signifying the importance of ferroelectric behavior of PVDF

Figure 25 depicts the complex dielectric permittivity dependence on frequency in a regular dielectric material. As the frequency increases the response of the dipole to the applied field decreases since regular dielectric materials have only low frequency dipolar polarization, which decays at higher frequencies starting from 1Mhz [28]. However, ferroelectric materials have high frequency dipolar polarization [28] that becomes active in this frequency range and tend to show improved polarization up to a frequency of 10E12Hz and there after only atomic or electronic polarization exist in a material. This is studied in COMSOL multiphysics by plotting polarization in the frequency range of 1Mhz to 10Ghz, which is shown in Figure 26.

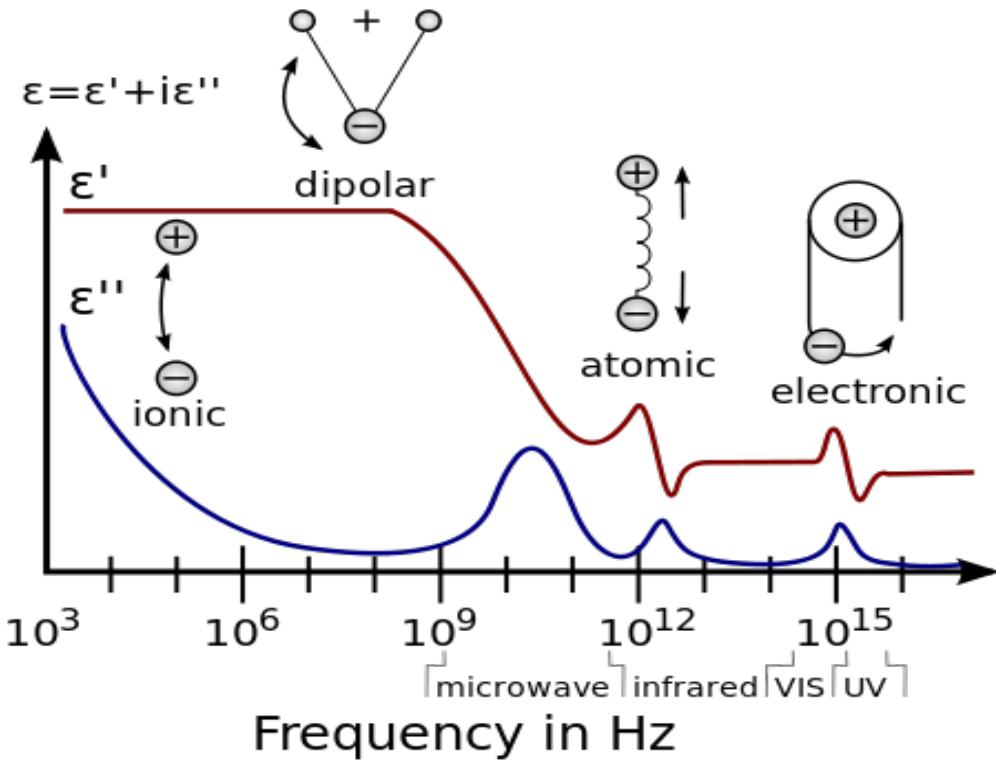

Figure 25. Dielectric permittivity spectrum of a regular dielectric material [26].

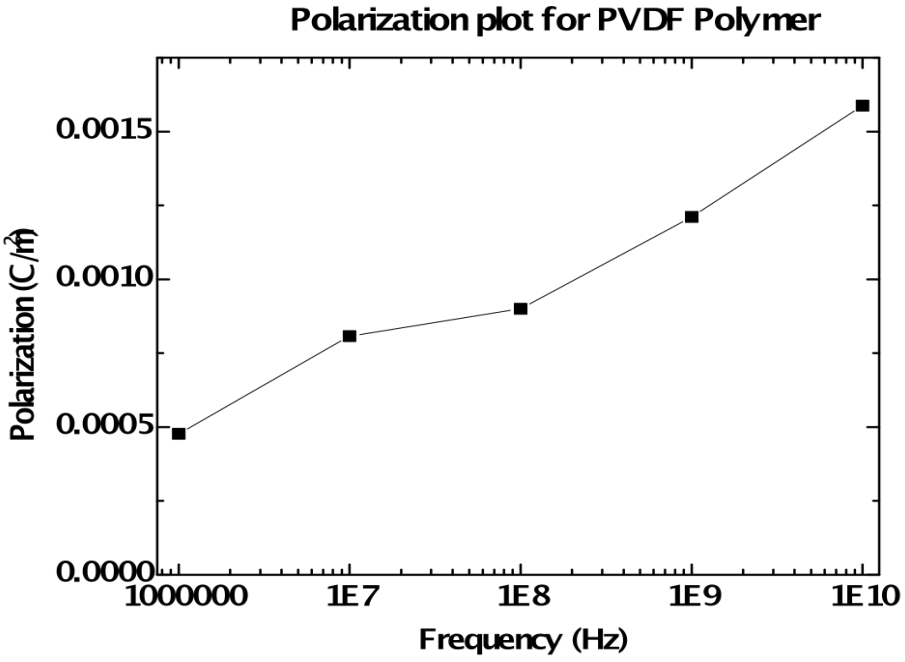

(a)

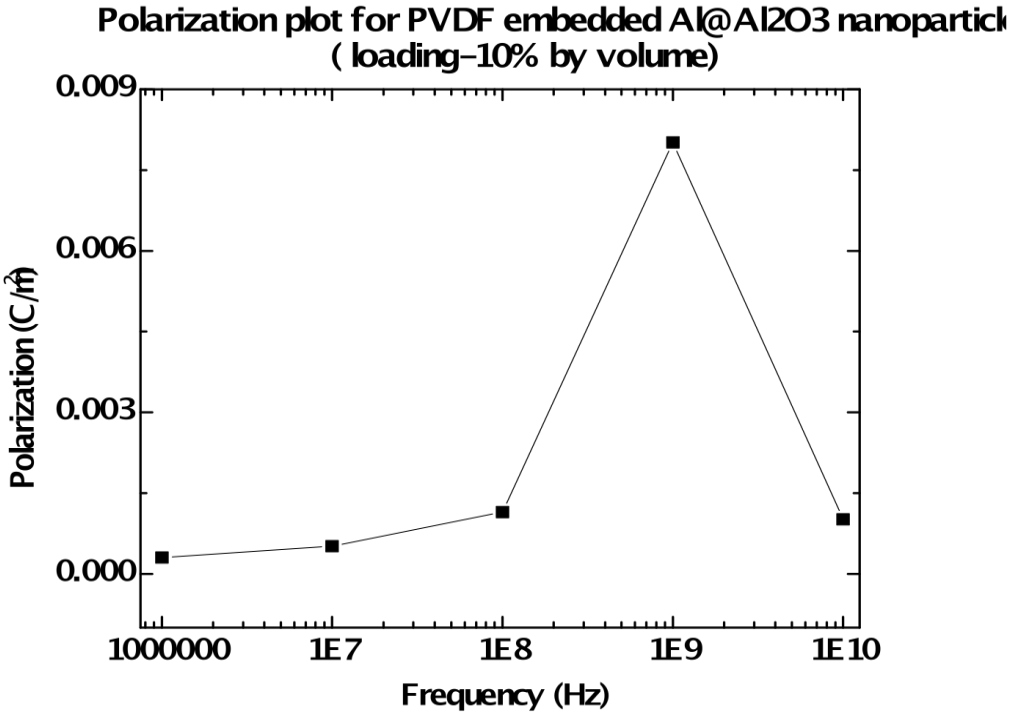

(b)

Figure 26. Polarization plot for a) PVDF, b) PVDF/Al@Al_2O_3 (10% loading) with varying frequency.

As noted above, the pure PVDF polymer, which is ferroelectric by nature, shows an increasing polarization from 5E-3 C/m^2 at 1E6HZ to 15E-3 C/m^2 at 1E10 Hz. When the polymer is embedded with $Al@Al_2O_3$ nanoparticles, polarization further increased to 80E-3 C/m^2 at 1E9 Hz from 0.3E-3 C/m^2 at 1E6Hz, and then drops to a value of 1.32E-3 C/m^2 at a frequency of 1E10 Hz. The reason for the decay in polarization might be due to inter particle oscillations that create higher dielectric loss, which reduces the polarization of composite medium. Thus, the ferroelectric polymer showed improved polarization at higher frequencies even when embedded with $Al@Al_2O_3$ nanoparticles.

CHAPTER 8: Conclusion and future work

8.1 Conclusions

A procedure has been developed to fabricate parallel plate capacitors with PVDF as a dielectric film and every step of the fabrication process has been optimized. Different loadings of nanoparticles were embedded into the PVDF polymer and its corresponding dielectric constant was calculated. It was observed that the dielectric constant K of the composite dielectric medium increased from 12 for pure PVDF polymer to a value of 23.6 when PVDF was embedded with a 20% loading of nanoparticles by volume. Frequency dependence of capacitance for fabricated capacitors with different loadings is also studied which gave a relatively constant response from 10KHz to 1MHz. Thermal characterization was carried out to study the variation of capacitance with temperature. It was observed that for PVDF polymer alone, and when embedded with nanoparticles of loading 10% and 20%, the PVDF gave a steady response until the temperature reached the PVDF pre melting point of 70^0C, and there after showed a steady decay with increase in temperature. Polymer with 20% loading showed a drastic drop in the capacitance after the pre melting point, which requires further study to understand the reason for this decay in capacitance. SEM analysis revealed a uniform nanodielectric film of thickness 6.34μm, which can be controlled by varying the concentration of polymer in the polymer solution. The XRD analysis confirmed the presence of Al_2O_3 along with Al inside the PVDF polymer that was found to have both β & γ phases. Table 5 shows the comparison of fabricated capacitors with other literature work.

Table 5: Comparison of fabricated capacitor with literature work

Materials	K	Tan δ	Filler Size	Filler loading	Ref.
$BaTiO_3$/epoxy	40 (1 Hz)	0.035 (1 Hz)	100-200nm	60 Vol%	29
Bimodal $BaTiO_3$	90 (100 kHz)	0.03 (100 kHz)	916nm+60	75 Vol%	30
Al/Ag-epoxy	160 (10 kHz)	0.045 (10 kHz)	Ag: <20nm	Al: 80 wt%	31
Au-SiO_2/PVP	20 (10 kHz)	0.08 (10 kHz)	35-60 nm Core-shell	64 Vol%	20
Al@Al_2O_3/PVDF	**23.6 (10 kHz)**	**0.0013 (10 kHz)**	**Al: 60 - 100nm Al_2O_3 – 15nm thick shell**	**20%**	**This Work**

From Table 5 it can be inferred that Al@Al_2O_3 fillers when embedded in PVDF polymer showed improved dielectric constant and very low dielectric loss with minimal loading of fillers as compared to the ceramic filler $BaTiO_3$ that gave high dielectric constant and dielectric loss with much higher loading of fillers. Also although the Au-SiO_2 core shell nanoparticle structure showed god response, it required many intermediate steps to functionalize an SiO_2 shell around expensive Au nanoparticles. This method not only makes the process costly but also has negative impact on the efficiency at which the capacitor dielectric is fabricated because of the introduction of additional chemicals at each stage of the functionalization process of the SiO_2 shell. There is also a possibility of the SiO_2 shell being ripped off the Au nanoparticles. Besides, the PVP polymer used is highly reactive with water and other solvents, which raises a great concern of its implementation for printed circuit boards. Hence, using Al nanoparticles with naturally formed Al_2O_3 shell embedded in PVDF polymer, which being chemically inert can greatly help to overcome the above mentioned disadvantages. Further the

Al@Al2O3 PVDF dielectric has a cost effective fabrication process and shows significant improvment of the dielectric constant with minimal dielectric loss at lower loading of fillers as compared to other literature work shown by Table5.

3D FEM simulations of the nanodielectric composites were performed through COMSOL Multiphysics with random distribution of nanoparticle. The dielectric function of PVDF polymer was calculated using the Drude model that displayed relatively constant dielectric value K with decay at higher frequencies because of increase in dielectric loss. Electric polarization and electric field patterns inside the dielectric were studied for increased loading of nanoparticles, and it was observed that the effective electric field around the composite medium decreased with increased polarization. Figure 27 illustrates the comparison of simulated values of the dielectric constant using percolation theory with experimental results.

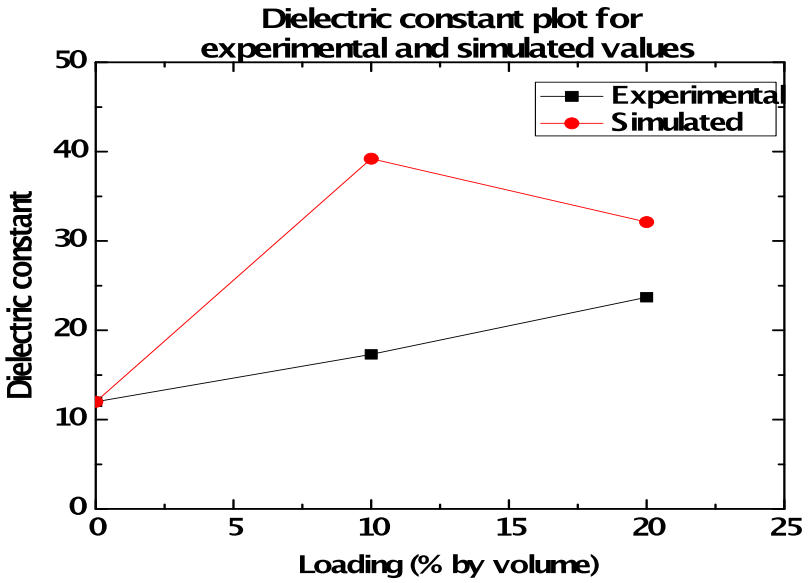

Figure 27. Comparison between simulation and experimental results for effective dielectric constant.

Difference with the results of Figure 26 is because percolation theory is a mathematical equation, which doesn't consider the materialistic properties and

interparticle behavior inside the medium that play a crucial role in practical nanodielectric composite. Hence, it was concluded that percolation theory could be used as a guide to get the loading fraction of nanoparticles that shows high dielectric constant in COMSOL simulations, which can be used as feedback for experimental work. Effective medium theory was also applied to understand the variation of K of nanodielectric composite with increase in frequency of applied potential. It was seen that the calculations followed experimental data shown in Figure 10 and further showed a relatively constant response up to a frequency of 10E12Hz and decay thereafter. Thus, EMT can be used as good approximation to predict the dielectric constant dependence on frequency at higher loadings. The polarization plot of PVDF and PVDF embedded with 10% loading of nanoparticles was also studied in the frequency range 1Mhz to 10Ghz to understand the behavior of the ferroelectric PVDF polymer at higher frequencies. Polarization was found to increase with frequency by a factor of 3 for bare PVDF polymer and by a much higher factor of 250 when embedded with nanoparticles over the frequency range of 1Mhz – 10Ghz. Also, decay in polarization from 80E-3 C/m^2 to 1.5 E-3 C/m^2 was observed in the polymer embedded nanoparticle composite, which requires further research to understand the reason for this decay. Thus, simulation results for polarization at higher frequencies helps us to realize that fabricated capacitors with PVDF ferroelectric polymer and $Al@Al_2O_3$ nanoparticles can be considered as a potential candidate to be used at higher frequencies and at higher voltages because of the high dielectric strength of the polymers compared to ceramic capacitors which are now being used at higher frequencies but with low operating voltage.

8.2 Directives for Future Work

This research can be extended to reach the target loading that can give a K value of 70, which is considered excellent in case of ferroelectric dielectric materials. This is possible by developing efficient ways to highly disperse nanoparticles into the polymer matrix with less agglomeration. Making the simulation more realistic by including boundary conditions at the interparticle interface, and by considering nanoparticles with varying sizes as observed in the SEM Figure 13, can give good direction to future experimental work. Further, the ferroelectric properties of the composite should be explored, which can be helpful in enhancing the dielectric properties of the nanocomposite and increasing the scope of application of fabricated capacitors at higher frequencies.

REFERENCES

1) Bourzac Katherine.,“ Nanocomposite Material Help Capacitors Pack a High Energy Punch ”, 2002.

2) Katherine Bourzac.,“ Nanopore Arrays Combine High Power and Storage Capacity”, March 16, 2009.

3) Tan1 Daniel and Irwin1 Patricia.,“ Polymer Based Nanodielectric Composites ”, April 2009.

4) Rajesh B., Nacer B. and Bensaoula A.,“ *Effective Medium Theory of Nanodielectrics for Embedded Energy Storage Capacitors* ”, COMSOL 2010 conference proceedings ISBN: 978-0-9825697-4-0, Newton, MA, October 7-9, 2010.

5) http://www.tf.uni-kiel.de/matwis/amat/elmat-en/kap-3/backbone/r3-5-1.html, 2004.

6) Averitt R.D., Sarkar D. and Halas N.J., “ Plasmon Resonance Shifts of Au-Coated Au2S Nanoshells: Insight into Multicomponent Nanoparticle Growth ”, Phys Rev Lett, Vol 78 No 22, June 1997.

7) www.radio-electronics.com/info/data/capacitor/capacitor_types.php*,* by Ian P., 2010.

8) Ulrich R.K. and Schaper.L.W,“ *Integrated Passive Component Technology* ”, IEEE press, Wiley-Interscience, New Jersey, 2003.

9) Lu J.,“ High Dielectric Constant Polymer Nanocomposites for Embedded Capacitor Applications ”, Georgia Institute of Technology, Georgia, 2008.

10) Shen Y., Lin Y., Li M., and Nan C.W.,“ High Dielectric Performance of Polymer Composite Films Induced by a Percolating Interparticle Barrier Layer ”, Adv. Mater, 19, 1418–1422, 2007.

11) http://www.goodfellow.com/E/Polyvinylidenefluoride.html, 2003.

12) Sataparthy S., Pawar S., Gupta P.K., Varma K.B.R.," Effect of Annealing on Phase Transition in Poly(vinylidene fluoride) Films Prepared Using Polar Solvent ", 2010.

13) Mathews Poulsen and Stephen Ducharme " Why Ferroelectric Polyvinylidene Fluoride is Special ", University of Nebreska, Nebreska, Lincoln, 2010.

14) http://www.americanelements.com/alnp.html, 2008.

15) Debye P.," Polar Molecules ", Published by Chemical Catalog Company, 1929.

16) Nan W, Shen Y and Jing Ma., " Physical Properties of Composites Near Percolation" ,Annu. Rev. Mater. Res. 2010. 40:3.1–3.21.

17) V. Myrochnychenko and C. Brosseau, " *Finite-Element Method for Calculation of the Effective Permittivity of Random Inhomogeneous Media* ", Physical Review E 71, 016701, 2005.

18) T.C .Choy, " Effective Medium Theory – Principles and Applications," Intrenational series of monographs on Physics, Oxford science publications, New York, 1999.

19) W. M. Merrill, R.E. Diaz, M. C. Squires and N. G. Alexopoulos, " Effective Medium Theories for Artificial Materials Composed of Multiple Sizes of Spherical Inclusions in a Host Continuum ", IEEE Transactions on antennas and propagation, vol. 47, no. 1, January 1999.

20) Bikky Rajesh," *Fabrication and Characterization of Polymer Based High-k Nano--dielectrics for Embedded Capacitor Applications* ", 2009.

21) "A study on Interfacial Adhesion of Poly(vinylidene fluoride) with Substrates in a Multilayer Structure ", published by Society of plastic engineers Inc, 2002.

22) Srivatsan T.S., " Processing and Fabrication of Advanced Materials ", XVII: Part 8: Polymer-based composites and nano composites: Volume Two.

23) http://www.omicsonline.org/scientific-reports/srep385.php,1998.

24) A Bourbia, S Boulkhessaim, H Bedboudi and M Draissia, " *Phase Transformation in Rapidly Solidified Al–Al2O3 Alloys by High-frequency Melting* ", 2002.

25) Zervos M, Tsokkou D, Pervolaraki M, Othonos A, " *Low Temperature Growth of In2O3and InN Nanocrystals on Si(111) via Chemical Vapour Deposition Based on the Sublimation of NH4Cl in In* " , May 2001 .

26) http://www.teehugger.com/renewable-energy/eestor-makes-tiny-annoucement-about-big-achievement.html, April 2009.

27) http://www.betelco.com/sb/phd/ch3/c34.html, 1998.

28) http://people.ee.ethz.ch/~fyuriy/oe/oe_optcom_chapters/Optoelectronics_2010_Ch02.pdf, 2010.

29) S. Liang, S. Chong and E. Giannelis, " *Barium Titanate/epoxy Composite Dielectric Materials for Integrated Thin Film Capacitors* ", Proceedings of the 48th Electronic Components and Technology Conference, pp. 171-175, 1998.

30) Q.M Zhang, V.Bharti and X. Zhao, " *Giant Electrostriction and Relax Ferroelectric Behavior in Electron-irradiated Poly(vinylidene fluoride-trifluofoethylenecopolymer Science* ", Vol. 280,pp.2101-2104,1998.

31) J. Lu, K. S. Moon and C. P. Wong, " *Development of Novel Silver Nanoparticles/ polymer Composites as High k Polymer Matrix by In-situ Photochemical Method* ", Proceedings of the 56th Electronic Components and Technology Conference, pp. 1841-1846, 2006.